



This is a repository copy of *Younger Dryas and Early Holocene ice-margin dynamics in northwest Russia*.

White Rose Research Online URL for this paper:

<https://eprints.whiterose.ac.uk/210119/>

Version: Published Version

Article:

Boyes, B.M. orcid.org/0000-0003-1309-2672, Pearce, D.M. orcid.org/0000-0002-6889-224X, Linch, L.D. orcid.org/0000-0002-9486-7574 et al. (1 more author) (2024) Younger Dryas and Early Holocene ice-margin dynamics in northwest Russia. *Boreas*, 53 (3). pp. 376-400. ISSN 0300-9483

<https://doi.org/10.1111/bor.12653>

Reuse

This article is distributed under the terms of the Creative Commons Attribution-NonCommercial (CC BY-NC) licence. This licence allows you to remix, tweak, and build upon this work non-commercially, and any new works must also acknowledge the authors and be non-commercial. You don't have to license any derivative works on the same terms. More information and the full terms of the licence here: <https://creativecommons.org/licenses/>

Takedown

If you consider content in White Rose Research Online to be in breach of UK law, please notify us by emailing eprints@whiterose.ac.uk including the URL of the record and the reason for the withdrawal request.



eprints@whiterose.ac.uk
<https://eprints.whiterose.ac.uk/>



Younger Dryas and Early Holocene ice-margin dynamics in northwest Russia

 BENJAMIN M. BOYES , DANNI M. PEARCE , LORNA D. LINCH  AND DAVID J. NASH 
BOREAS

 Boyes, B. M., Pearce, D. M., Linch, L. D. & Nash, D. J.: Younger Dryas and Early Holocene ice-margin dynamics in northwest Russia. *Boreas*. <https://doi.org/10.1111/bor.12653>. ISSN 0300-9483.

The dynamics of the last Fennoscandian Ice Sheet (FIS) are relatively well constrained in the Nordic countries. Ice-sheet dynamics in NW Russia, however, are comparatively less well understood owing to the scale and resolution of existing studies. New large-scale glacial geomorphological datasets from NW Russia based on high-resolution remotely sensed imagery allow for an independent reassessment of the extent and dynamics of the FIS during the Younger Dryas and Early Holocene (*c.* 12.9–10 ka) in NW Russia. The reconstruction provides a more detailed link between geomorphological expressions of palaeoglaciation than previous proposals. Rather than a continuous Younger Dryas ice marginal zone (IMZ) stretching from Finland to northern Norway, the geomorphological signature of NW Russia reveals 14 IMZs that document discrete stationary ice-margin positions (possibly standstill and/or readvance events) during the overall retreat. The relative age sequence of the IMZs, supported by an updated numerical age database, suggests that they formed time-transgressively during the Younger Dryas and Early Holocene rather than contemporaneously. Moreover, specific landform assemblages reveal contrasting glacial landsystems in NW Russia: (i) a northern subpolar glacial landsystem; and (ii) a southern temperate glacial landsystem. The model presented herein provides robust empirical constraints for testing and validating numerical ice-sheet models and understanding ice-sheet responses to rapid climate change.

Benjamin M. Boyes (b.boyes@sheffield.ac.uk), Department of Geography, University of Sheffield, Sheffield S10 2TN, UK and School of Applied Sciences, University of Brighton, Lewes Road, Brighton BN2 4GJ, UK; Danni M. Pearce, Faculty of Environmental Science and Natural Resource Management, Norwegian University of Life Sciences, Postbox 5003, 1433 Ås, Norway; Lorna D. Linch, School of Applied Sciences, University of Brighton, Lewes Road, Brighton BN2 4HP, UK; David J. Nash, School of Applied Sciences, University of Brighton, Lewes Road, Brighton BN2 4HP, UK and School of Geography, Archaeology and Environmental Studies, University of the Witwatersrand, Private Bag 3, Wits 2050, Johannesburg, South Africa; received 6th April 2023, accepted 2nd February 2024.

The Younger Dryas stadial (*c.* 12.9–11.7 ka) was the last period of climatic cooling during the Late Weichselian (*c.* 40–10 ka) glaciation (Rasmussen *et al.* 2014; Mangerud 2021). Notably, the Younger Dryas terminated rapidly with an abrupt climatic warming in the order of several degrees Celsius during the Younger Dryas–Early Holocene transition *c.* 11.7 ka (Rasmussen *et al.* 2014). In response to these abrupt climatic shifts, the Fennoscandian Ice Sheet (FIS) is thought to have responded dynamically and subsequently collapsed (Andersen *et al.* 1995a; Stroeven *et al.* 2016; Mangerud 2021). Investigating such abrupt palaeoclimatic shifts, including reoccurrence and magnitude, is crucial for future projections of climate change and subsequent ice-sheet response.

To understand ice-sheet dynamics during the Younger Dryas stadial, successive studies have focussed on the lateral extent of the FIS (e.g. Lavrova 1960; Andersen 1979; Punkari 1985; Ekman & Iljin 1991; Lundqvist 1995; Rainio *et al.* 1995; Andersen *et al.* 1995b; Mangerud *et al.* 2016; Johnson *et al.* 2019), which is often defined by the last major zone of ice-marginal landforms in Fennoscandia (Fig. 1; Andersen *et al.* 1995a; Stroeven *et al.* 2016). The FIS Younger Dryas ice marginal zones (IMZs; defined here as ice marginal landform assemblages including morainic and

meltwater landforms indicative of stationary ice-margin positions) have been mapped almost continuously throughout Fennoscandia (Lundqvist 1995; Rainio *et al.* 1995; Andersen *et al.* 1995a, b). This suggests that the climatic cooling of the Younger Dryas impacted the entire FIS. However, the landforms within the Younger Dryas IMZs reveal distinct local variations in the ice sheet. In Norway, the FIS margin was predominantly located in a fjord landscape, which resulted in a highly crenulated ice margin of fjord glaciers bounded by terrestrially based ice (Andersen *et al.* 1995b; Mangerud *et al.* 2016, 2019; Stroeven *et al.* 2016). In addition, several ice caps, plus cirques and small valley glaciers, glaciated some of the Norwegian upland landscape at the margins of the FIS (Bakke *et al.* 2005; Wittmeier *et al.* 2020; Regnéll *et al.* 2022). Elsewhere, the FIS margin terminated as arcuate ice lobes on lowland terrain (Punkari 1980, 1982, 1985; Lundqvist 1995; Putkinen & Lunkka 2008; Stroeven *et al.* 2016).

Although the Younger Dryas IMZs in Norway, Sweden and Finland are largely well constrained (Andersen *et al.* 1995a; Stroeven *et al.* 2016), their position in NW Russia (Fig. 1), and thus the maximum Younger Dryas FIS extent, are somewhat uncertain. For example, on the Kola Peninsula, Boyes *et al.* (2021a) identify four conflicting Younger Dryas ice-sheet reconstructions

currently advocated by the literature (Fig. 1C), including: *et al.* 1993; Yevzerov & Nikolaeva 2000; Yevzerov 2001); (i) crenulated FIS margins with ice lobes occupying topographic depressions (Ekman & Ijijin 1991; Niemela extending into the White Sea (Yevzerov & Kolka 1993;

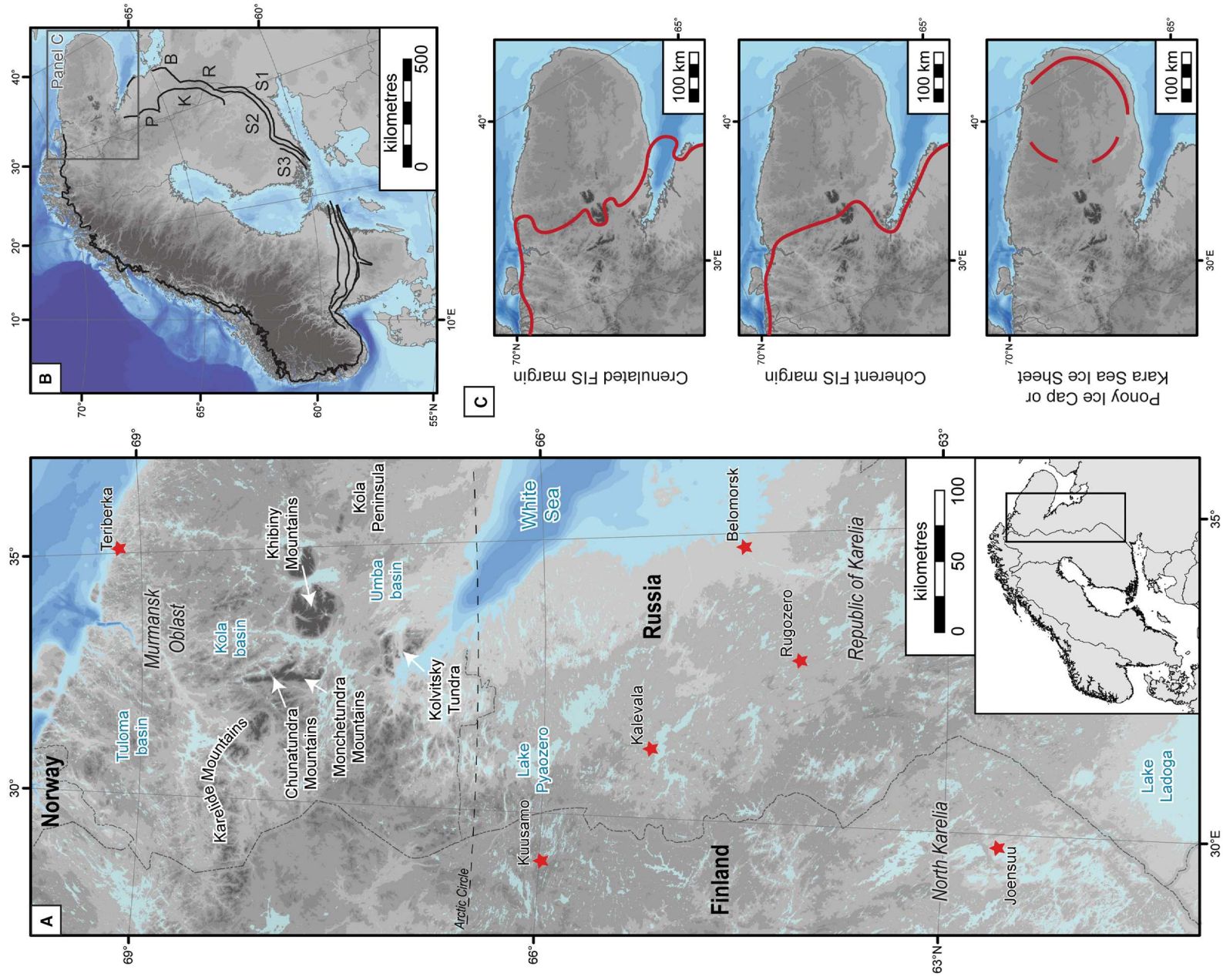


Fig. 1. A. The study area of NW Russia, including place names mentioned in the text. B. Ice marginal zone (IMZ) positions (dark grey lines) attributed to the Younger Dryas stadial extent of the FIS (modified from Hughes *et al.* 2016). IMZs in Karelia and Finland are labelled as follows: P = Pyaozero; B = Belomorsk; K = Kalevala; R = Rugozero; S1 = Salpausselkä I; S2 = Salpausselkä II; S3 = Salpausselkä III. C. Alternative Younger Dryas IMZs on the Kola Peninsula (red lines), including (top) a crenulated FIS margin, (middle) a coherent FIS margin, and (bottom) IMZs associated with different ice masses. In this and subsequent figures, topography and bathymetry data are from the European Space Agency (2021) and GEBCO Compilation Group (2023). The topography is shaded dark–light grey with darker shades representing higher ground; the bathymetry is shaded dark–light blue with darker shades representing greater depth.

Hättestrand & Clark 2006b; Hättestrand *et al.* 2008; Stroeven *et al.* 2016); (iii) FIS glaciation on the western Kola Peninsula and Ponoj Ice Cap glaciation on the eastern Kola Peninsula (Ekman & Iljin 1991; Rainio *et al.* 1995; Svendsen *et al.* 2004; Astakhov *et al.* 2016; Lunkka *et al.* 2018); and (iv) glaciation by the Kara Sea Ice Sheet (Grosswald 1980, 2001; Grosswald & Hughes 2002). These reconstructions are largely based on small-scale Quaternary geological data. For example, some studies have generalized, extrapolated and interpolated local-scale high-resolution data (e.g. Lavrova 1960; Niemelä *et al.* 1993; Petrov *et al.* 2014), while other studies have been unable to identify smaller features in low-resolution (decametre) satellite imagery (e.g. Punkari 1982, 1985, 1995; Hättestrand & Clark 2006a). Using such small-scale data has the potential to propagate into incorrect or overgeneralized interpretations. For example, Boyes *et al.* (2021a) argue that by using generalized small-scale geological data, proponents of the Ponoj Ice Cap overlook regional geomorphological signatures that would lead to alternative interpretations.

However, despite being based on small-scale Quaternary geological data, IMZ reconstructions in the Republic of Karelia are generally consistent (Fig. 1B). Large arcuate landform assemblages dominated by end moraines, glaciofluvial ridges and deltas are often grouped into two discrete IMZs (Kurimo 1982; Punkari 1982, 1985, 1993, 1995; Ekman & Iljin 1991; Rainio *et al.* 1995; Boulton *et al.* 2001; Putkinen & Lunkka 2008; Putkinen *et al.* 2011; Yevzerov 2018). The outermost IMZs, the Rugozero and Belomorsk (Fig. 1B), are widely regarded as continuations of the Salpausselkä II moraine in Finland (Punkari 1982, 1985; Ekman & Iljin 1991; Rainio *et al.* 1995; Stroeven *et al.* 2016) and are often attributed to the Younger Dryas stadial (Rainio *et al.* 1995; Stroeven *et al.* 2016). The inner IMZs, the Kalevala and Pyaozero (Fig. 1B), are often correlated with the Salpausselkä III moraine in Finland (Punkari 1980, 1982, 1985; Rainio 1985; Ekman & Iljin 1991; Rainio *et al.* 1995; Stroeven *et al.* 2016). These innermost IMZs are thought to be temporary ice-sheet responses to the Preboreal oscillation (a short cooling period *c.* 11.4 ka) after the Younger Dryas stadial (Rainio *et al.* 1995; Stroeven *et al.* 2016). Although there is a wealth of research on FIS retreat patterns in Karelia, there has been little critique of the relative timing of IMZ formation in the study area. This is despite, for example, Putkinen (2011) hypothesizing asynchronous formation of the Karelian

IMZs. As noted previously, using small-scale geological data can lead to overgeneralized interpretations, including the relative ages of IMZs. Thus, it is pertinent to reconsider IMZ reconstructions in NW Russia.

In this study, we utilize extensive large-scale glacial geomorphological data derived from high-resolution (sub-decametre) remotely sensed data to re-assess palaeoglaciological evidence of Younger Dryas and Early Holocene deglaciation patterns and dynamics in NW Russia. The aim is to (i) independently identify the most likely Younger Dryas FIS extent on the Kola Peninsula and (ii) test existing Younger Dryas IMZ reconstructions in Karelia. Additionally, this study will re-assess regional- and local-scale ice-margin dynamics in NW Russia. This new palaeoglaciological reconstruction provides an evidence-led assessment that can be used for targeting field investigations of ice-margin dynamics, and for testing and validating numerical ice-sheet and climate models.

Material and methods

Ice-margin reconstruction

The methods for reconstructing IMZs and ice-margin retreat patterns follow the glacial inversion approach (Kleman & Borgström 1996; Clark *et al.* 2012; Stokes *et al.* 2015). Large-scale mapping by Boyes *et al.* (2021b) and Boyes and Pearce (2023) identified >128 000 morainic and meltwater landforms in the study area from high-resolution remotely sensed imagery, which have a spatial resolution of up to 2 m. The extent of the datasets used for landform identification – the ArcticDEM Digital Surface Model, PlanetScope Ortho Scene data and Esri World Imagery – is explained in Boyes *et al.* (2021b) and Boyes and Pearce (2023). These geomorphological data are the principal components of the ice-margin reconstruction (Figs 2, 3). However, the large volume of individual geomorphological data needs to be reduced to manageable and meaningful pieces of summary information to facilitate the inversion of a glacial geomorphological map (Fig. 2) (Clark *et al.* 2012; Boyes *et al.* 2023b). Such summaries are then used to reconstruct ice-margin positions (Fig. 2). To ensure that the ice-margin reconstruction is as robust as possible, morainic and meltwater landforms identified with the lowest confidence in the Boyes *et al.* (2021b) and Boyes and Pearce (2023) datasets are excluded. This

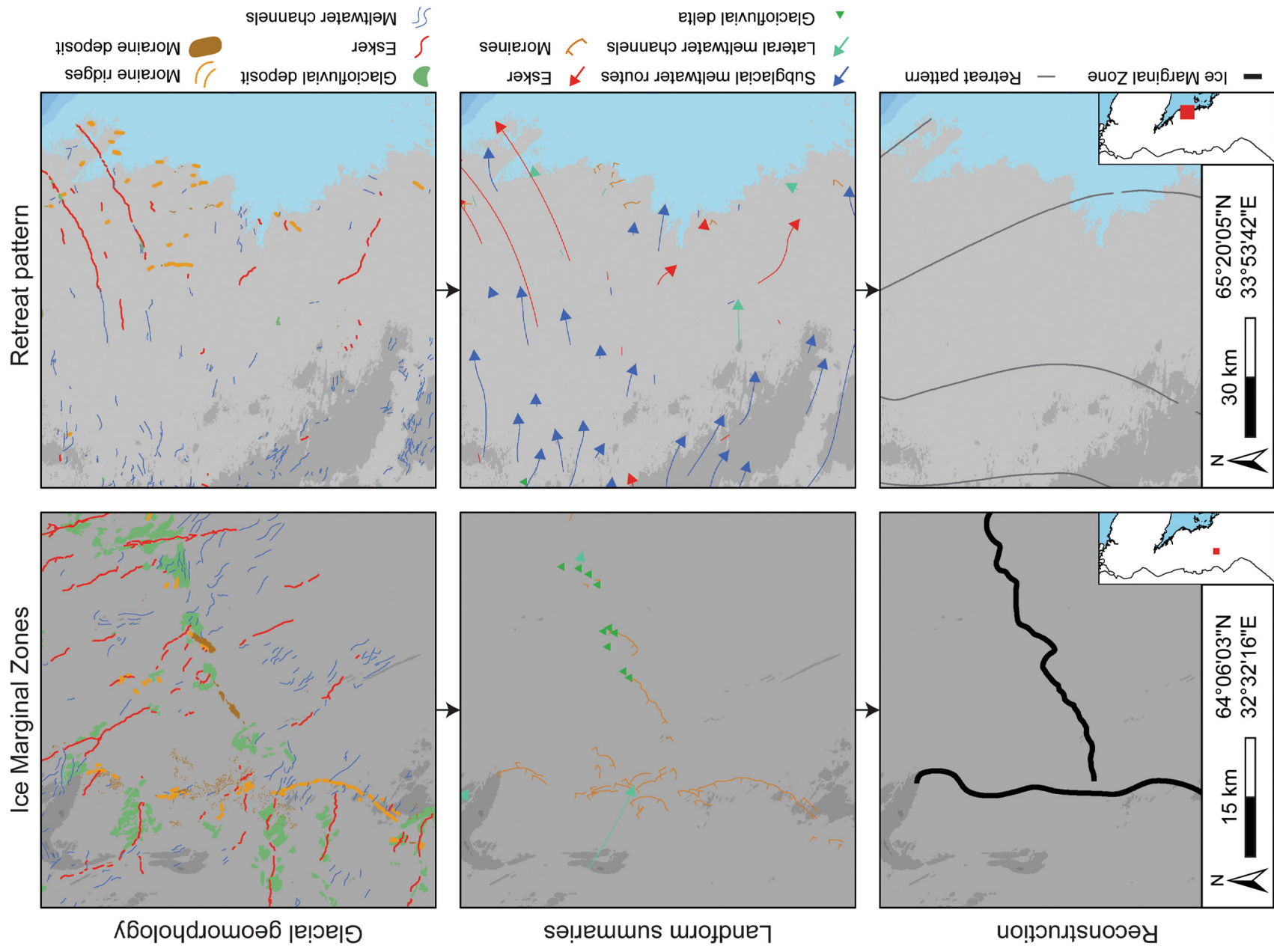


Fig. 2. The method by which individual geomorphological data mapped by Boyes *et al.* (2021b) and Boyes and Pearce (2023) are used to reconstruct IMZs and ice-sheet retreat patterns. First, individual geomorphological data (top panels) are synthesized into landform summaries that document ice-flow direction and/or ice-margin positions (middle panels), which are subsequently used to reconstruct IMZs and ice-sheet retreat patterns (bottom panels). The IMZ reconstructions (left panels) are based only on ice-marginal landforms (moraines, lateral meltwater channels and glaciofluvial deltas), whereas retreat patterns (right panels) draw on the entire landform assemblage.

reduces landform data by ~1.2% across the entire region, but does not, in our opinion, affect the interpretation of the geomorphological record.

Summaries of morainic and meltwater landforms are generated following Boyes *et al.* (2023b). Moraines are summarized by a single line representing the inferred ice-margin position. Glaciofluvial delta apices are summarized as points and the maximum lateral extent of ice-dammed lakes is reconstructed to infer ice contact slopes. Eskers, lateral and subglacial meltwater channels, and Type 3 hummocky moraine corridors (which are irregular mounds thought to be remnants of subglacial meltwater drainage networks; Boyes *et al.* 2021b) are first summarized as arrows in the inferred direction of ice flow, and then as deglaciation patterns perpendicular to the inferred ice flow direction. In this study, we do not use the subglacial bedform record as this information is not strictly required for reconstructing the position of IMZs and deglaciation patterns (Hättestrand & Clark 2006b; Clark *et al.* 2012; Dulfer *et al.* 2022).

Subsequently, the landform summaries are used to reconstruct (i) the position of IMZs revealed by, for example, grouped assemblages of moraines and glaciofluvial deposits, and (ii) the most likely ice-sheet retreat pattern by combining the resulting inferred ice-flow directional data and ice-margin positions to produce an overall regional summary. This approach allows the identification of disparities and agreements between the different landforms. Where data are sparse, ice margins are extrapolated across the landscape on the basis of topographic setting and the principle of morphostratigraphy. In areas of complex topography and where data are especially sparse, margins are left unconnected to avoid erroneous interpretations. Since the geomorphological data used in this study were compiled using the same (i) remotely sensed data sources, (ii) mapping methods within a Geographic Information System (GIS), and (iii) diagnostic landform identification and classification criteria (Boyes *et al.* 2021b; Boyes & Pearce 2023), the reconstruction is consistent across the entire study area.

Establishing a chronological framework

Establishing a chronological framework involves two stages: (i) identifying relative age relationships between discrete landform assemblages; then (ii) assigning a numerical chronology. Determining a relative chronology of IMZ formation follows the principle of

morphostratigraphy. Landforms typically develop in a sequence alongside a retreating ice margin. Thus, IMZ proximity to the centre of a palaeo-ice sheet can be used to establish relative age. In some cases, ice margins can readvance and rework or overlap pre-existing landform assemblages. Where overlapping IMZs are observed, the features that have been superimposed or reworked are interpreted as older features. Following these principles and by careful examination of landform relationships (using the high-resolution (2 m) digital surface model used for mapping), IMZs are arranged into a relative age stack.

To assess the absolute chronology of glaciation in the study area, the numerical age database presented in Boyes *et al.* (2023b) has been expanded to include numerical ages ≤ 150 km outside and beyond the study area. These data were prepared for use within a GIS and are available to download in the Supporting Information (see Data S1–S3). A census date of October 2022 is applied to this database; any dates published after this are not included. The database now contains 245 radiocarbon ($n = 129$), terrestrial cosmogenic nuclide (TCN; $n = 57$), optically stimulated luminescence (OSL; $n = 57$), and palaeomagnetic ($n = 2$) dates derived from glacial and non-glacial investigations that are relevant to the Late Weichselian glaciation (e.g. basal radiocarbon dates from Holocene climate reconstruction studies).

The methods for compiling this database, assigning glaciodynamic and reliability classifications to the individual dates, and applying the database to the reconstruction follow Boyes *et al.* (2021a, 2023b) and Boyes (2022), and are summarized here. Coordinates are reported in decimal degrees and the WGS84 datum, following the recommendations of Hughes *et al.* (2016). To maintain consistency across the dataset and enable site-to-site comparisons, numerical ages are recalculated and/or recalibrated where appropriate (refer to Boyes *et al.* 2021a for further details). Radiocarbon ages – which are recalibrated using the INTCAL20 (Reimer *et al.* 2020) or Marine20 (Heaton *et al.* 2020) calibration curves for present-day terrestrial and marine sampling locations, respectively – are reported here as cal. ka BP (i.e. before 1950). The TCN, OSL and palaeomagnetic ages are reported relative to the year of sampling/analysis (ka) following standard conventions. A consistent datum is not imposed across dates derived from different methods since the maximum deviation between dates is negligible in comparison with the timescales involved within the reconstruction.

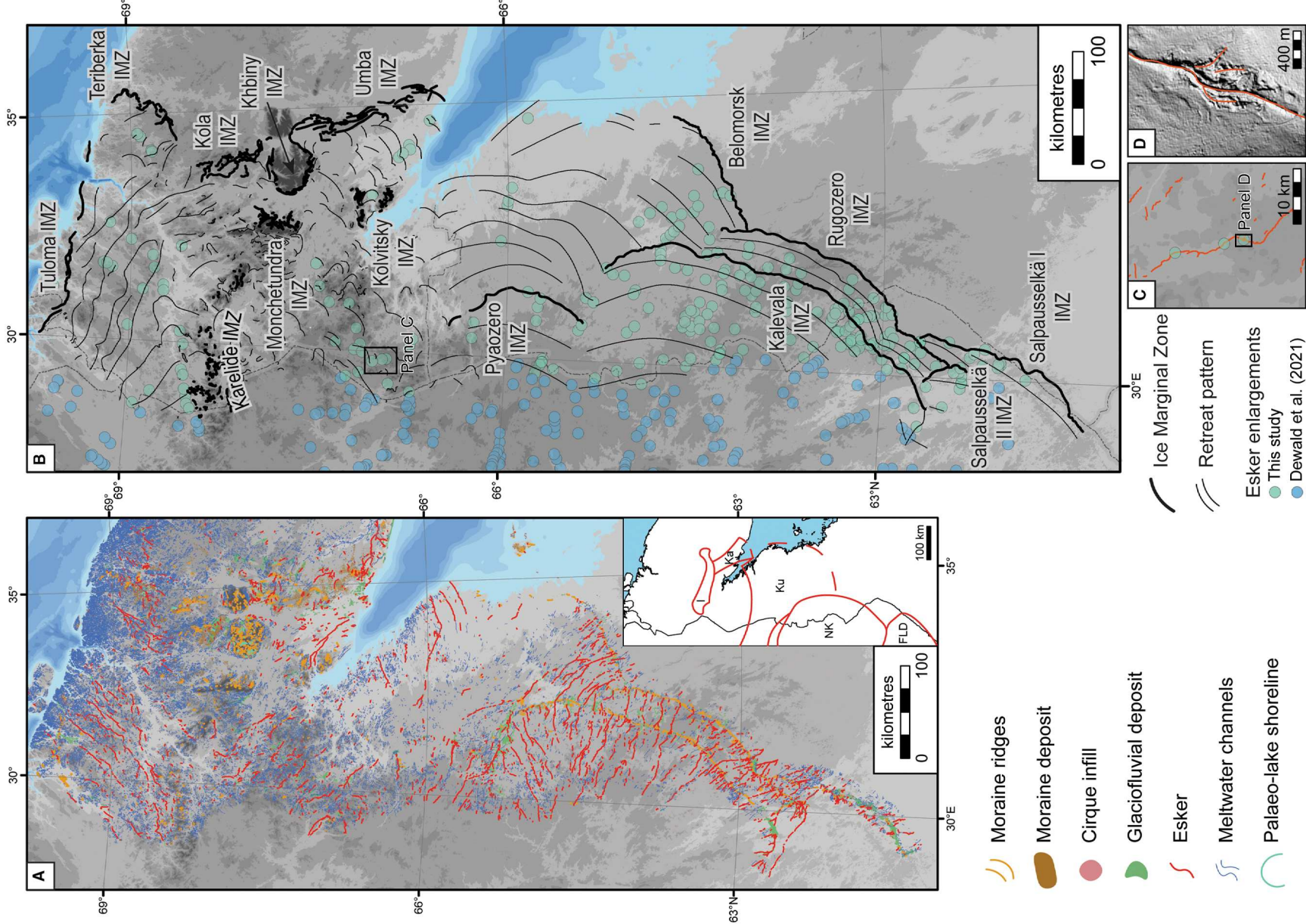


Fig. 3. Geomorphological data and the reconstructed IMZs and ice-sheet retreat patterns in NW Russia and bordering Finland. A. Medium- and high-confidence geomorphological data used in this study (modified from Boyes *et al.* 2021b and Boyes & Pearce 2023). Low-confidence landforms, which were not used in this study, and are not shown. To view these data in detail, the reader is directed to Boyes *et al.* (2021b) and Boyes and Pearce (2023) where the data can be downloaded in GIS shapefile format. The symbology of the geomorphology in this figure is used in the subsequent figures of this paper. These data are used to identify the IMZs and retreat pattern in (B). Inset: ice lobes (ice streams) in the study area as defined by Lunkka *et al.* (2021) and Boyes *et al.* (2023b). I = Imandra ice lobe; Ka = Kanozero ice lobe; Ku = Kuusamo ice lobe; NK = North Karelian ice lobe; FLD = Finnish Lake District ice lobe. (B) Reconstructed IMZs and ice-sheet retreat patterns in the study area. Ice-margin positions on the Kola Peninsula and Russian Lapland are modified from Boyes *et al.* (2023b). Names for the IMZs are derived from the geographical location of the landform assemblages. Locations of esker enlargements identified in this study and neighbouring eastern Finland (modified from Dewald *et al.* 2021) are also shown. Panel (C) details the position of esker enlargements along individual eskers, and (D) shows an example of an esker enlargement from ArcticDEM imagery. Abundant esker enlargements in the study area may indicate a rapidly retreating ice margin.

The geomorphological and sedimentary context provided in the source publication from which individual dates are retrieved is recorded for each date in Data S1 and S2. This information is used to determine the glaciodynamic context and reliability of the dates. To derive the glaciological meaning of the individual numerical ages, dates were classified following the procedure of Bryson *et al.* (1969) and Hughes *et al.* (2016) into the following categories: advance, deglacial, margin, ice-free and exposure time (cumulative). Some dates cannot be classified owing to improper reporting in the source publication (i.e. the dates are not provided with contextual or stratigraphical information or data for calibrating radiocarbon dates). Such dates are reported as N/A in Data S1 and S2.

Advance dates (e.g. from OS�-dated glaciofluvial sediments buried beneath till deposits) indicate that the ice cover at a particular location occurred after the given age and can be used to constrain the advance of the ice sheet. Deglacial dates (e.g. from post-glacial sediments overlying tills) indicate ice-free conditions at a location before the given age. Where ages are derived from sediments located between two tills, the date is classified as an advance date in reference to the upper till unit as it represents the most recent glacial event (but it is noted that the date may also be a deglacial date for the lower till). The date could also constrain an oscillating ice margin rather than the initial advance of an ice sheet, although a date from beneath the lower till would be needed to confirm this. A margin date (e.g. from *in situ* TCN dated boulders along the crest of a moraine ridge) is identified where there is reason to consider that the ice margin was close by. Ice-free dates (e.g. from radiocarbon dated basal lake sediments) indicate non-glacial (i.e. ice-free) conditions that occurred before or after glaciation, thus providing an age bracket for glaciation at a location. Finally, exposure time (cumulative) dates indicate relict bedrock or boulder surfaces that are preserved beneath cold-based ice and are derived solely from TCN dating.

The following criteria – including (i) the quality of the contextual, stratigraphical, and sample property information reported in the source publication, (ii) comments concerning the reliability of the date in the source publication, (iii) the location of the sample site in relation to the mapped landforms presented in Boyes *et al.*

(2021b) and Boyes and Pearce (2023), and (iv) the relationship of the date to other published dates from the same site – were used to categorize each date into one of three reliability classes:

- Reliable (3) – date provided with full contextual, stratigraphical and sample property information. Glaciodynamic interpretation is deemed to be correct.
- Possibly reliable (2) – date provided with some contextual, stratigraphical and sample property information. Glaciodynamic interpretation may be incorrect.
- Unreliable (1) – date provided with no contextual, stratigraphical and sample property information. Glaciodynamic interpretation may be incorrect.

Reliable and possibly reliable numerical ages are then assigned to the IMZ reconstruction and deglaciation pattern. Before assigning ages to the reconstruction, it is important to note that there are large areas of the study area that are devoid of dates, that in some cases there is disagreement between dates from surrounding areas and that many numerical ages in the study area are not targeted at palaeoglaciological events. This hinders attempts to interpret the spatial and temporal evolution of the FIS across the entire region. The ages are, therefore, assigned to selected ice-margin positions, and in many cases can only be extrapolated across relatively short distances to reduce introducing further uncertainties to the overall reconstruction. Most of the assigned dates are minimum ages, meaning that the margin is at least that age and could be older. However, if a margin is known to fall between two or more dates, an age range is given.

Results

Morainic and meltwater landforms are mapped across the study area (Fig. 3B). Belts of hummocky and end moraines, in places up to 35 km wide, and large spreads of glaciofluvial sediments (up to 84 km²) are typically arranged in arcuate assemblages on lowland terrain. Hummocky and end moraines are also distributed across valley floors in mountainous regions of Murmansk Oblast. Meltwater channels are similarly found in a

variety of settings, including across lowland terrain, perched on valley sides and superimposed on other glacial landforms. In contrast, eskers are predominantly found on lowland terrain, often forming trails over 100 km long. For full geomorphological descriptions, see Boyes *et al.* (2021b) and Boyes and Pearce (2023).

Ice marginal zones and deglaciation pattern

The reconstructed IMZs and retreat pattern are presented in Fig. 3B. The reconstruction is restricted to contemporary terrestrial surfaces by a lack of offshore data that precludes, for example, a reconstruction of retreat patterns in the White Sea. Fig. 3A also shows the ice lobes, which may have been active as ice streams, reconstructed by Lunkka *et al.* (2021) and Boyes *et al.* (2023b), that were probably associated with the IMZs and retreat pattern. In total, 14 IMZs are identified from the geomorphology in the study area (Fig. 3B; Table 1). These are defined by assemblages of ice-marginal deposits (i.e. moraines and glaciofluvial deposits) and indicate standstills and/or readvances of the ice-margin position during the overall retreat (Fig. 2). In contrast, ice-sheet retreat patterns are revealed by the spatial distribution of glacial landforms that may not necessarily indicate a standstill and/or readvance of the ice margin (e.g. esker longitudinal axes) but were formed during the overall retreat of the ice sheet (Fig. 2). The 14 IMZs (Fig. 3B, Table 1) are named after their geographical location. In some cases, multiple names for discrete IMZs or fragments of IMZs exist across the published literature: when this occurs, we have chosen to use names that reflect their contemporary setting. Additionally, we identify 215 instances of esker enlargements (Dewald *et al.* 2021) in the study area (Fig. 3B), whereby eskers undergo morphological changes from a single ridge to a braided complex of ridges and glaciofluvial sediments and back to a single ridge. The majority of these features (>75%) are located proximal to the IMZs in Karelia.

Relative ages of ice-marginal zone formation

The IMZs and retreat patterns presented in Fig. 3B reveal a spatial record of glaciation in NW Russia. The next stage of the interpretation is to identify the temporal dimension and establish the relative timings of deglaciation. Figure 3B achieves this in part by showing the most recent (i.e. the last) ice-margin position. For example, on the Kola Peninsula, it is likely that the outermost and adjacent IMZs – Tuloma, Teriberka, Kola, Khibiny, and Umba – are of similar relative age based on their morphostratigraphical distribution. Other IMZs in NW Arctic Russia were probably formed during subsequent ice-sheet retreat. However, other morphostratigraphic relationships between discrete IMZs in Karelia reveal a more complex relative age sequence.

Evidence of possible obliterative overlaps – where cycles of ice-margin retreat and advance rework evidence of previous ice-margin positions (Gibbons *et al.* 1984; Kirkbride & Winkler 2012; Barr & Lovell 2014) – in Karelia suggests that the formation of discrete IMZs was asynchronous (Fig. 4). For example, at the confluence of the Belomorsk and Rugozero IMZs (Fig. 4) the discrete IMZs and ice flow patterns (revealed by the subglacial meltwater channel and esker orientations) are almost perpendicular. Moreover, the end moraines within the Rugozero IMZ display only proximal ice contact slopes. This suggests that the Belomorsk IMZ was formed before the Rugozero IMZ and that the ice margin had retreated before forming the Rugozero IMZ during an overlapping flow event. Similarly, almost perpendicular IMZs displaying only proximal ice-contact slopes and converging ice-flow patterns (revealed by the subglacial meltwater channel and esker orientations) at the meeting of the Rugozero and Salpausselkä II IMZs (Fig. 4) indicate that the Salpausselkä II IMZ formed after the retreat of the Rugozero IMZ. Contrastingly, the Salpausselkä I and Rugozero IMZs are subparallel to each other. However, >30 km of overlapping landform assemblages and end moraine ridges at the northern end of the Salpausselkä I IMZ that arc into an almost perpendicular orientation to the Rugozero IMZ (Fig. 4) indicate that the two IMZs cannot have formed synchronously.

An obliterative overlap interpretation at the confluence of the Salpausselkä II and Kalevala IMZs is more complex. Perpendicular landform assemblages may be indicative of asynchronous formation. However, at the southern limit of the Kalevala IMZ is a glaciofluvial delta with both a proximal and a (possible) distal ice contact slope (Fig. 4), although postglacial wave erosion has significantly reworked the Salpausselkä II side of the delta. Moreover, an interlobate moraine and esker system feeds into the western side of this delta deposit (Fig. 4). This indicates that the glaciofluvial delta may have been deposited in a space between two adjacent ice margins and suggests that the Salpausselkä II and Kalevala IMZs may have formed synchronously.

Absolute chronology of deglaciation

The glacial landform evidence from NW Russia reveals a sequence of events that has been used to piece together a relative chronology of ice-margin evolution – this information is presented in Table 2. To tie the relative chronology to an absolute chronology of events, 245 previously published numerical ages are compiled into a numerical age database (Fig. 5). Metadata and critical assessments of each age can be viewed in Data S1 and S2, but additional discussion is provided as necessary below.

Numerical ages are assigned to the IMZs from the most reliable (medium and high confidence) numerical dates. In Norway, TCN ages associated with the Tuloma IMZ indicate that this ice margin was established *c.*

12.4–11.0 ka (DATABASE_ID 189–198). This is supported by basal radiocarbon dates from lake cores on the proximal side of the Tuloma IMZ that indicate ice-free conditions *c.* 10.5 cal. ka BP (DATABASE_ID 2–7). Elsewhere in Murmansk Oblast, basal radiocarbon dates from lake cores located on the proximal sides of the Teriberka, Khibiny and Umba IMZs indicate an initiation of ice-free conditions *c.* 11.5 cal. ka BP (DATABASE_ID 21–22, 72, 222). This timing is contradicted by bulk organic radiocarbon dating of glacial varves ~45 km behind the Umba ice margin on the White Sea coastline (Kolka *et al.* 2013b), where ages indicate an ice margin as early as 13.2 ± 0.7 cal. ka BP (DATABASE_ID 12–13). However, these ages do not consider a marine reservoir effect that may have resulted in an erroneously older age. We therefore use radiocarbon ages on the Kola Peninsula cautiously and suggest that the outermost belts of IMZs – the Teriberka, Kola, Khibiny and Umba IMZs – formed concurrently before *c.* 11.5 cal. ka BP.

Direct numerical age estimations for the Monchetundra, Kolvitsky and Karelide IMZs are absent. Minimum limiting ages for the Monchetundra and Kolvitsky IMZs may be provided by basal radiocarbon dates from a lake core ~12 km south of the Monchetundra massif (DATABASE_ID 73–74). Tolstobrova *et al.* (2016) present diatom assemblages from the lake core, which suggest deposition of sediments in a proglacial environment 11.3 ± 0.8 and 11.2 ± 0.6 cal. ka BP; for this to be the case, both the Monchetundra and Kolvitsky IMZs would have to be deglaciated prior to this time. Thus, our best estimate is that the Monchetundra and Kolvitsky IMZs were formed prior to *c.* 11.3 cal. ka BP. A minimum limiting age for the Karelide IMZ is provided by a single radiocarbon age of a peat deposit (DATABASE_ID 92), which suggests organic accumulation 10.5 ± 0.4 cal. ka BP. Therefore, our best age estimate for the Karelide IMZ is formation prior to *c.* 10.5 cal. ka BP.

Numerical ages in Karelia are similarly patchy and the majority (>70%) are ice-free ages, meaning that they can only provide minimum age constraints. Within the study area, there are no numerical ages targeted at the Salpausselkä I IMZ. Lunkka *et al.* (2021) present an OSL age (13.3 ± 0.9 ka) from the Sairakkala delta, which is associated with the western arc of the Salpausselkä I IMZ. However, considering the apparent time-transgressive formation of IMZs in Karelia, we are cautious about assigning this age to the Salpausselkä I IMZ within our study area. We therefore tentatively suggest that the Salpausselkä I IMZ in Karelia may have been established by the start of the Younger Dryas stadial, in keeping with interpretations by Stroeven *et al.* (2016) and Lunkka *et al.* (2021). Radiocarbon dates from basal lake organic sediments within the Belomorsk IMZ (DATABASE_ID 233–234) indicate the initiation of ice-free conditions at 12.0 ± 0.2 and 11.9 ± 0.2 cal. ka BP. This is supported by further basal organic lake sediment radiocarbon ages on the proximal

side of the Belomorsk IMZ (DATABASE_ID 226–232). This suggests that the Belomorsk IMZ was formed prior to *c.* 12.0 cal. ka BP. Moreover, we tentatively suggest that the Belomorsk IMZ formed in tandem with the Salpausselkä I IMZ; this is because the relative age sequence (Table 2) indicates that the Belomorsk and Salpausselkä I IMZs are both older than the Rugozero IMZ. However, targeted numerical age estimations are required to verify this interpretation. Numerical age estimations for the Rugozero IMZ that may help this interpretation are currently lacking.

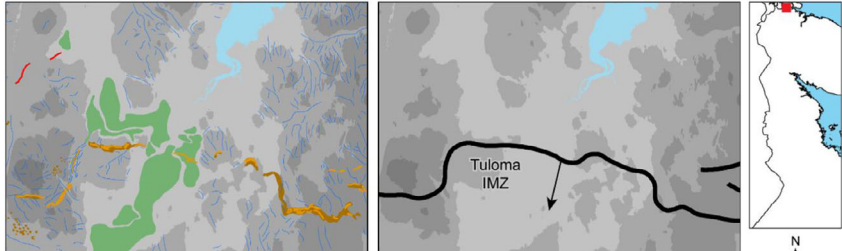

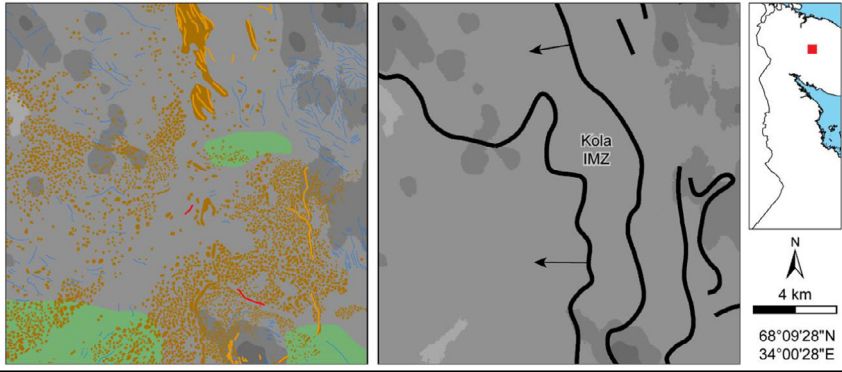
Within the study area, there are no numerical ages targeted at the Salpausselkä II IMZ, but OSL ages in Finland (DATABASE_ID 240 and 244) suggest that this ice margin was established between 12.0 and 11.8 cal. ka BP. Although the relative age sequence suggests that the Kalevala IMZ may have formed concurrently with the Salpausselkä II IMZ (Table 2), existing numerical ages are not conclusive. Putkinen *et al.* (2011) provide three palaeomagnetic ages to support glacial varve data from the region surrounding the Kalevala IMZ. However, we only include the palaeomagnetic age estimation from Lake Ala-Kuittijärvi in our database (DATABASE_ID 44) because (i) the authors regard this sediment succession, which is on the proximal side of the Kalevala IMZ, to be the most complete and representative of the earliest ice-free conditions, and (ii) we cannot verify the number of glacial varves to estimate an earlier age. Thus, the current best estimate for the formation of the Kalevala IMZ is before 10.9 cal. ka BP.

Constraining the timing of the Pyaozero IMZ currently relies on distal and proximal numerical ages. Approximately 14 km east of the Pyaozero IMZ (DATABASE_ID 177), radiocarbon dating of gyttja indicates ice-free conditions 10.9 ± 0.2 cal. ka BP, suggesting that underlying varved clays were deposited prior to *c.* 10.9 cal. ka BP. Supporting this age estimation, radiocarbon dating of basal lake sediments ~20 km west on the proximal side of the Pyaozero IMZ suggests that the IMZ was ice free by 10.2 ± 0.1 cal. ka BP (DATABASE_ID 41). As such, our best estimate for the timing of the Pyaozero IMZ is before *c.* 10.9 cal. ka BP.

Discussion

Large-scale glacial geomorphological mapping, synthesis and interpretation has been applied to NW Russia to develop our understanding of the Younger Dryas and Early Holocene FIS in the region. The resulting IMZ and retreat pattern reconstruction (Fig. 3B, Table 2), which is discussed here, is argued to best fit the landform legacy of glaciation. This reconstruction is grounded, qualitatively, in assumptions of glacial geomorphological processes and guided by analogues from contemporary ice sheets and other palaeo-ice sheets. This discussion is followed by suggestions for future research in the region.

Table 1. Names and geomorphological characteristics of the ice-marginal zones (IMZs) identified in this study. The IMZs are named after their geographical location. In some cases, previous studies have used alternative names for an entire IMZ or part of an IMZ – where this occurs, the alternative name and selected publications are provided for reference only. Examples of the characteristic glacial geomorphology mapped by Boyes *et al.* (2021b) and Boyes and Pearce (2023) (using the same symbology as Fig. 3) and the IMZ reconstruction (thick black lines with arrows pointing up-ice) are also shown.

Ice marginal zone (alternative name; example publication)	Geomorphological characteristics	Example (left: geomorphological mapping from Boyes <i>et al.</i> (2021b) and Boyes and Pearce (2023)) (right: interpreted IMZ)
Tuloma	End moraine ridges on the bedrock scoured, fjord-like terrain of northern Russian Lapland and northern Norway. In the example (right), the end moraine ridges demarcate the ice-sheet margin position on higher ground and an outlet glacier extending ~3 km into a valley.	
Teriberka	Arcuate assemblages of ring and ridge (Type 2a; Boyes <i>et al.</i> 2021b) hummocky moraines in places bounded by end moraine ridges. In the example (right), the arcuate landform assemblage is observed in lower topography, whereas a recess in the margin position occurs on higher ground.	
Kola	Large spreads of ring and ridge hummocky moraines and glaciofluvial outwash deposits with scattered end moraine ridges. In the example, IMZ positions are identified from end moraine ridges and the maximum extent of ring and ridge hummocky moraines.	

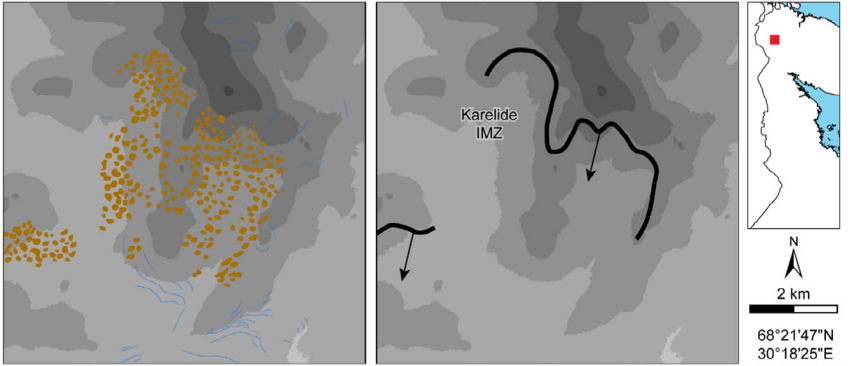
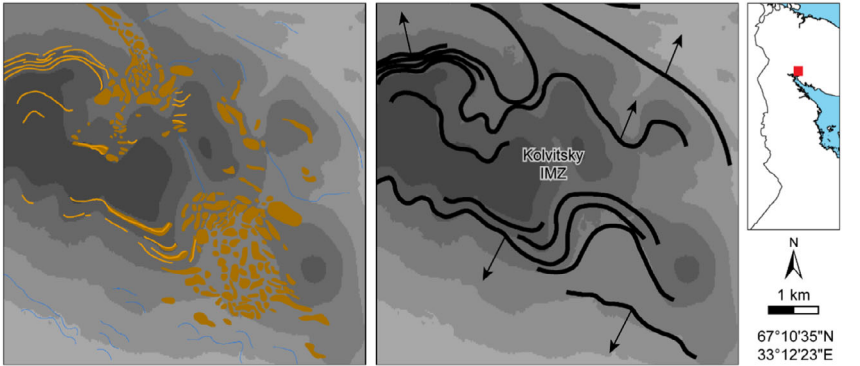
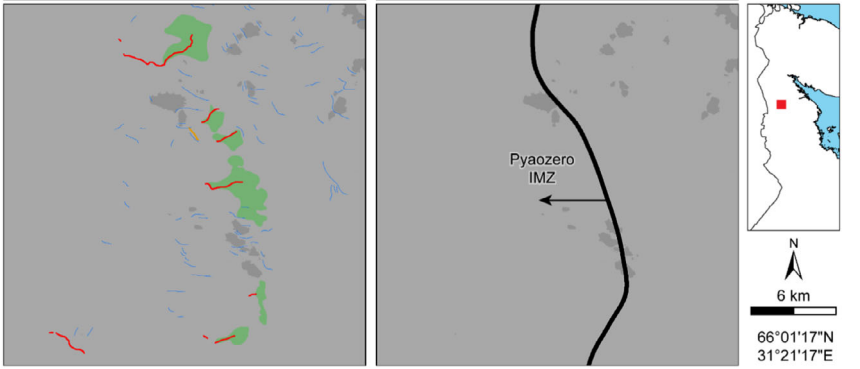
(continued)

Table 1. (continued)

Ice marginal zone (alternative name; example publication)	Geomorphological characteristics	Example (left: geomorphological mapping from Boyes <i>et al.</i> (2021b) and Boyes and Pearce (2023)) (right: interpreted IMZ)
Khibiny	Lateral moraines flanking the Khibiny massif and large cross-valley end moraines at valley mouths. In the example (right), a large cross-valley end moraine blocks the entrance to the Khibiny Mountains. On the mountain slopes, IMZ positions are indicated by narrow lateral moraine ridges and lateral meltwater channels.	
Umba	North-south aligned IMZ between Lake Umbozero and the White Sea is dominated by ring and ridge hummocky moraines interspersed with end moraine ridges. Prominent end moraine ridges and distal glaciofluvial outwash deposits are located at the downstream extent of the Imandra Ice Stream (Fig. 2; Boyes <i>et al.</i> 2023b) at the northern end of the Umba IMZ. In the example (right), the IMZ position is interpreted from the large spread of ring and ridge hummocky moraines and prominent end moraine ridges.	
Monchetundra	Lateral moraines, and ring and ridge (Type 2a) and irregular mound (Type 2b; Boyes <i>et al.</i> 2021b) hummocky moraines on the eastern flanks of the Monchetundra and Chunutundra Mountains. In the example (right), the landform assemblage and reconstructed IMZ indicates a glacier occupying a topographic depression and flowing around topographic highs.	

(continued)

Table 1. (continued)

Ice marginal zone (alternative name; example publication)	Geomorphological characteristics	Example (left: geomorphological mapping from Boyes <i>et al.</i> (2021b) and Boyes and Pearce (2023)) (right: interpreted IMZ)
Karelide	<p>Concentrated spreads of ring and ridge hummocky moraines across generally south-facing valley floors.</p> <p>In the example (right), the distribution of ring and ridge hummocky moraines and occasional lateral meltwater channels indicates an ice margin retreating down-valley (i.e. from higher to lower elevations).</p>	
Kolvitsky	<p>Lateral moraines stacked on mountain slopes and irregular mound (Type 1a; Boyes <i>et al.</i> 2021b) hummocky moraines spread across valley floors in the Kolvitsky Tundra.</p> <p>In the example (right), the distribution of hummocky moraines, lateral moraines and occasional lateral meltwater channels indicates a thinning ice-sheet and an ice margin retreating down-valley (i.e. from higher to lower elevations).</p>	
Pyaozero (Pääjärvi; Putkinen <i>et al.</i> 2011)	<p>A radial assemblage of eskers terminating in a prominent, arcuate assemblage of glaciofluvial deltas.</p> <p>In the example (right), a belt of glaciofluvial deltas with proximal eskers and surficial lateral/proglacial meltwater channels are interpreted as the IMZ.</p>	

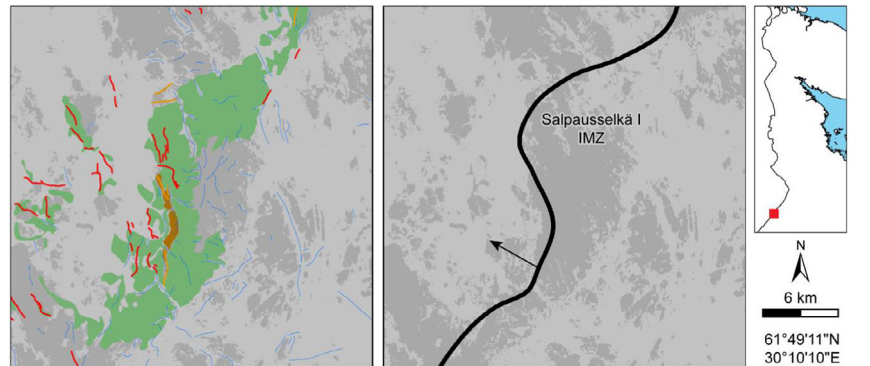
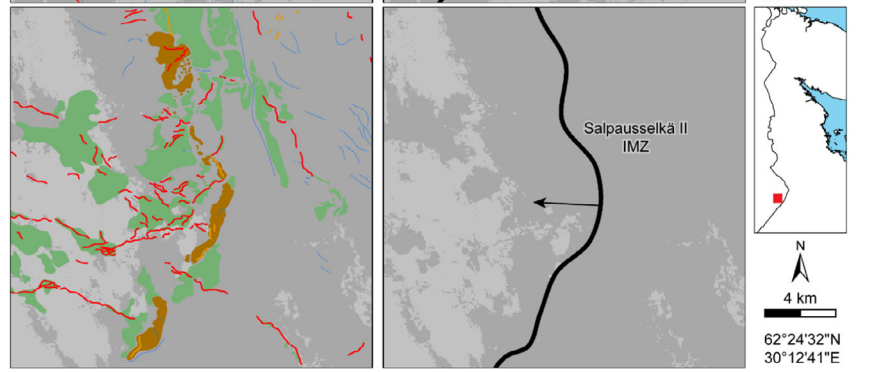
(continued)

Table 1. (continued)

Ice marginal zone (alternative name; example publication)	Geomorphological characteristics	Example (left: geomorphological mapping from Boyes <i>et al.</i> (2021b) and Boyes and Pearce (2023)) (right: interpreted IMZ)
Belomorsk	Discontinuous end moraines and glaciofluvial deltas form a west–east aligned arcuate IMZ. Occurrences of moraines and outwash deposits decrease eastwards as the Belomorsk IMZ reaches the White Sea coastline. In the example (right), discontinuous end moraine ridges with scattered eskers and subglacial meltwater channels demarcate the IMZ.	
Rugozero (Koitere; Rainio 1985)	Narrow end moraine ridges <35 m high and scattered ring and ridge hummocky moraines. A prominent glaciofluvial delta deposit toward the southern limit of the Rugozero IMZ (62°52'08\"/>	
Kalevala (Pielisjärvi or Jaamankangas; Rainio 1985)	An approximately north–south aligned arcuate landform assemblage characterized by narrow end moraine ridges <35 m high, scattered ring and ridge hummocky moraines, and glaciofluvial outwash deposits. In the example (right), eskers and subglacial meltwater channels end at end moraine ridges interspersed with glaciofluvial outwash deposits and occasional glaciofluvial deltas.	

(continued)

Table 1. (continued)

Ice marginal zone (alternative name; example publication)	Geomorphological characteristics	Example (left: geomorphological mapping from Boyes <i>et al.</i> (2021b) and Boyes and Pearce (2023)) (right: interpreted IMZ)
Salpausselkä I (Tuupovaara; Rainio 1985)	<p>Within the mapped area, the Salpausselkä I IMZ is characterized by end moraines and prominent glaciofluvial delta and outwash deposits.</p> <p>In the example (right), the IMZ is reconstructed at the proximal ice contact slope of prominent glaciofluvial deltas and interspersed end moraine ridges.</p>	
Salpausselkä II	<p>Within the mapped area, the Salpausselkä II IMZ is characterized by end moraines and prominent glaciofluvial delta and outwash deposits.</p> <p>In the example (right), the IMZ is reconstructed along end moraine ridges and glaciofluvial deltas, which are interspersed with numerous eskers and glaciofluvial outwash deposits.</p>	

Deglaciation pattern and timing

From the reconstructed IMZs and retreat pattern (Fig. 3B), contrasting and time-transgressive retreat patterns are apparent across NW Russia. Moraines and meltwater landforms in the study area indicate regional and local variations in retreat patterns during the Younger Dryas–Early Holocene glaciation. The largest contrast in ice-margin geometry occurs between Karelia and Murmansk Oblast (Fig. 3B). In Karelia, the arcuate assemblages that characterize the IMZs appear to disregard topography, suggesting that the geometry of the FIS dictated the pattern of retreat. However, IMZs have a crenulated appearance at landform scales, suggesting that thin ice margins were somewhat topographically deflected. In contrast, in Murmansk Oblast, the position of upland areas appears to have manipulated the pattern of ice-sheet retreat and forced outlet glaciers to retreat down-valley, i.e. from higher to lower elevations. Lateral meltwater channels near the summits of upland areas in Murmansk Oblast document ice-sheet thinning (Greenwood *et al.* 2007; Boyes *et al.* 2021b, 2023b), which would initially have exposed highpoints in northern parts of the study area as nunataks. The Khibiny, Karelide, Monchetundra and Kolvitsky IMZs are characterized by topographically defined moraine and glaciofluvial deposits, suggesting that subsequent ice-sheet thinning in upland areas delineated the FIS margin and encouraged a down-valley glacier retreat pattern (Heyman & Hättestrand 2006; Boyes *et al.* 2023b). Moreover, moraines flanking the Khibiny Mountains suggest that the massif forced a recess in the FIS margin during the Younger Dryas stadial.

The morphostratigraphic relationships between discrete IMZs across the study area reveal a complex relative age sequence (Fig. 3B, Table 2). In Karelia, this is similar to that presented previously by Putkinen (2011). However, despite compiling a comprehensive database of previously published numerical ages, we find that many dates for the study area are not targeted at discrete IMZs and/or glacial events. This precludes attempts to assign a robust absolute chronology to IMZs in NW Russia. Moreover, the spatial and temporal distribution of numerical ages in the study area precludes interpretations of Late Weichselian and Early Holocene ice-sheet retreat rates. Thus, despite previous estimates in the study area (e.g. Boulton *et al.* 2001; Putkinen 2011; Stroeven *et al.* 2016), it is difficult to confidently estimate the rate of ice-margin retreat.

The IMZ geometry and ice-sheet retreat pattern presented here is generally consistent with NW Russia deglaciation scenarios presented by Punkari (1980, 1982, 1985), Rainio *et al.* (1995), Ekman and Iljin (1991), Boulton *et al.* (2001), Putkinen *et al.* (2011), Yevzerov (2018) and Boyes *et al.* (2023b), among others. However, our revised IMZ and retreat pattern reconstruction (Fig. 3B) adds considerable detail to

previous reconstructions. For example, we have been able to identify crenulated forms of Karelian IMZs when using large-scale mapping and reconstruction approaches, which contrasts with previous reconstructions that demonstrate more even appearances derived from small-scale geomorphological data (e.g. Punkari 1982; Ekman & Iljin 1991; Boulton *et al.* 2001; Yevzerov 2018). Crucially, an assessment of the relative timing of IMZ formation is now well established. Rather than a continuous and synchronous >1000 km-long western FIS margin (e.g. Ekman & Iljin 1991; Rainio *et al.* 1995; Boulton *et al.* 2001; Stroeven *et al.* 2016; Yevzerov 2018), we find that the Younger Dryas IMZs in NW Russia were formed time-transgressively (Table 2), thus supporting the previous interpretation by Putkinen (2011). Moreover, contrasting landform assemblages are identified between neighbouring IMZs, suggesting distinct ice-sheet dynamics in the region. Below, we discuss some of these aspects and analyse their implications for ice-sheet dynamics.

Dynamic, topographic and climatic controls on ice-margin positions

From the geomorphological record of IMZs (Fig. 3), we infer that the FIS margin underwent a sustained readvance or periodic standstill during the Younger Dryas stadial in NW Russia. However, the maximum extent of the FIS during this period was not attained at the same time, and the morphologies of each IMZ are diverse. This suggests that different sectors of the FIS experienced unique controls behind their margin response. For example, on lowland landscapes, spreading and divergent ice flow facilitated surge-type events (Kleman *et al.* 1997). Arcuate IMZs in Karelia are generally characterized by (i) a distal zone of glaciofluvial outwash deposits and proglacial meltwater channels, (ii) an intermediate zone of end moraines and glaciofluvial deltas, and (iii) a proximal zone of ring and ridge (Type 2a; Boyes *et al.* 2021b) hummocky moraines and abundant subglacial meltwater channels and eskers (Table 1). Subglacial lineations also dominate the proximal landform record (Punkari 1982, 1985; Kleman *et al.* 1997, 2006). Similar landform assemblages in Latvia and Iceland have been interpreted as readvancing or surging glacier landsystems (Evans *et al.* 2007, 2009; Bitinas 2012; Schomacker *et al.* 2014; Lamsters & Zelčs 2015). Sedimentary and landform evidence from the Salpausselkä IMZs in Finland, including fluted surfaces of glaciotectionized glaciofluvial sediments (Salonen 1990; Lunkka *et al.* 2021), support the interpretation that IMZs were formed during readvance and flow reorganization events, although sedimentary evidence from NW Russia is absent. Thus, IMZs in Karelia are cautiously interpreted as maximum stationary ice-margin positions of glacier readvance events during the Younger Dryas–Early Holocene glaciation.

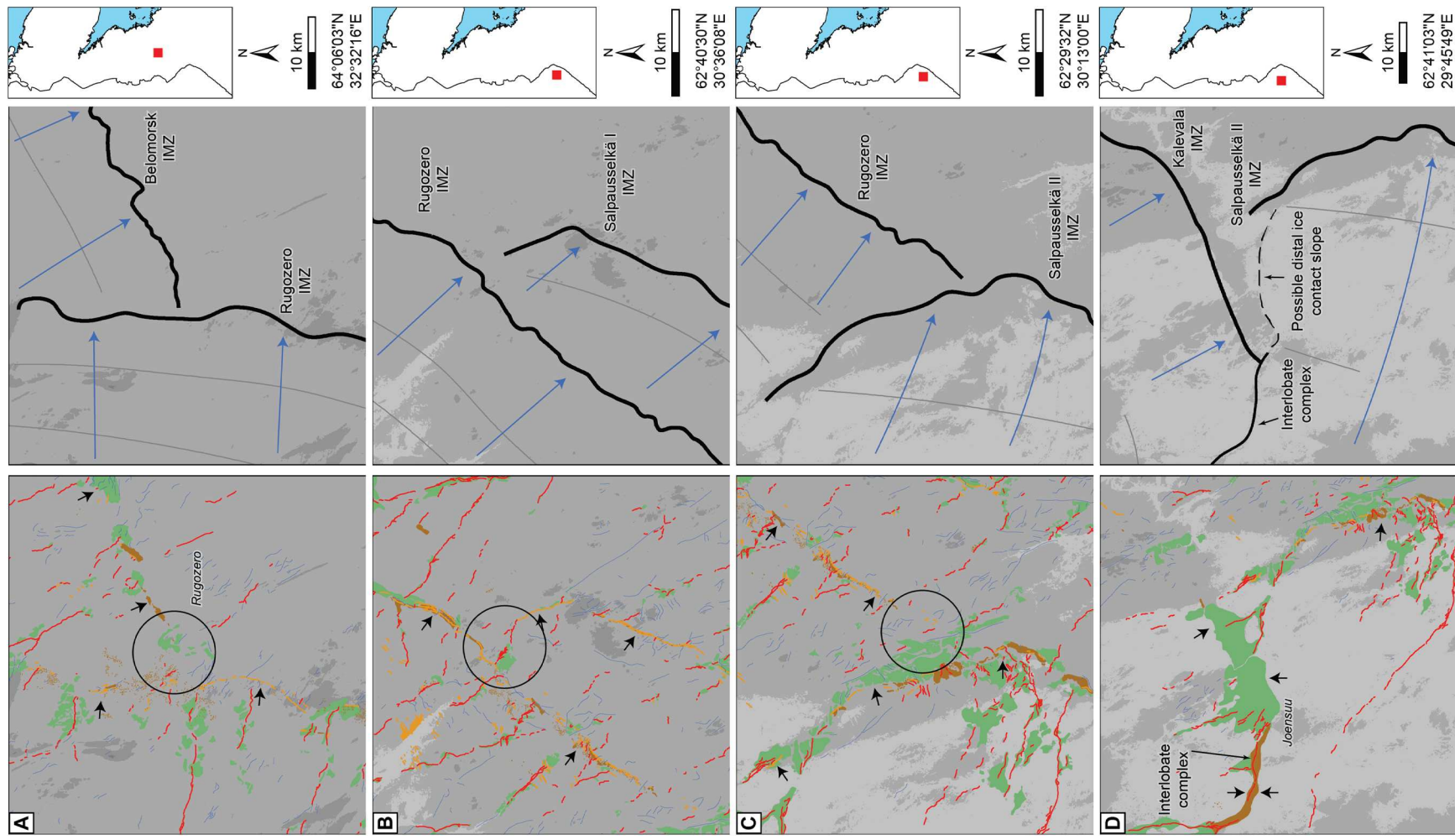


Fig. 4. Morphostratigraphy of the landform assemblages in Karelia suggests that IMZ formation was asynchronous. The symbology of the landforms in the left panels matches Fig. 3, the black arrows indicate ice contact slopes, and black circles outline perpendicular landform assemblages. In the right panel, IMZs are represented by thick black lines, thin grey lines are retreat patterns and blue arrows indicate the ice flow direction interpreted from the subglacial meltwater networks. Concertina-like landform assemblages (left panels) are interpreted as evidence of obliterative overlap events, where glacial readvances rework evidence of previous ice-margin positions. Thus, the reconstructions (right panels) reveal a concertina-like pattern of ice-sheet retreat where (A) the Rugozero IMZ forms after the Belomorsk IMZ, (B) the Rugozero IMZ forms after the Salpausselkä I IMZ and (C) the Salpausselkä II IMZ forms after the Rugozero IMZ. In (D) two ice contact slopes on a large glaciofluvial delta and an interlobate complex between converging ice lobes suggest that, despite overlapping IMZs, the Salpausselkä II and Kalevala IMZs may have formed synchronously.

The morainic and meltwater landform assemblage in Karelia also suggests that the Kuusamo, North Karelian and Finnish Lake District ice lobes – which were probably operating as ice streams (Fig. 2; Stroeven *et al.* 2016; Lunkka *et al.* 2021; Boyes *et al.* 2023a) – were probably active in a temperate glacial landsystem (Evans & Twigg 2002). The warm-based thermal regime of this landsystem produces three characteristic depositional domains in the geomorphological record of the study area. First, extensive end moraines, which in some cases can display sequences of stacked ice-marginal landforms, indicate stationary ice margins (Evans & Twigg 2002; Darvill *et al.* 2017; Kurjański *et al.* 2021). Second, large ice marginal glaciofluvial deltas, outwash deposits often in the distal zone of IMZs and abundant subglacial meltwater drainage features in the proximal zone indicate subglacial discharge of meltwater and debris in a warm-based temperate glacial landsystem (Punkari 1997; Evans & Twigg 2002; Evans & Orton 2015; Darvill *et al.* 2017; Kurjański *et al.* 2021). This suggests that ice lobes were driven by subglacial meltwater lubrication rather than a cooling climate. Finally, only scattered instances of hummocky moraine spreads in the proximal zone of Karelian IMZs indicate that widespread ice stagnation was uncommon (Evans & Twigg 2002; Darvill *et al.* 2017). The similarity between the landform assemblages in our study area and those associated with temperate glaciers supports the assertion that the ice lobes predominantly operated under a temperate glacial landsystem.

On the Kola Peninsula, abundant ring and ridge (Type 2a; Boyes *et al.* 2021b) hummocky moraines – which display complex ring, ridge, and hummocky morphologies

(Fig. 6) – dominate the Teriberka, Kola and Umba IMZs and may also be indicative of ice-margin readvances. The debris inputs for this type of moraine must be supraglacial, subglacial or englacial (Hoppe 1952; Gravenor & Kupsch 1959; Johnson *et al.* 1995; Mollard 2000; Boone & Eyles 2001). However, supraglacial debris is unlikely across most of NW Arctic Russia owing to the absence of high bedrock cliffs above much of the ice-sheet surface (this would preclude the supply of extraglacial rock debris). Thus, debris must have had either subglacial or englacial origins. Two possible formation models for these moraines have been proposed. First, the ring and ridge hummocky moraines form from water-saturated subglacial sediments that are squeezed into basal cavities under glacial ice (Hoppe 1952; Gravenor & Kupsch 1959; Johnson *et al.* 1995; Mollard 2000; Boone & Eyles 2001; Evans 2009; Yevzerov 2015; Vashkov & Nosova 2019). Alternatively, the moraines could be accumulations of previously englacial debris later exposed and accumulated at the surface of a stagnant, down-wasting ice margin (Fig. 6; Gravenor & Kupsch 1959; Aartolahti 1974; Lagerbäck 1988; Sollid & Sørbel 1988; Johnson *et al.* 1995; Mollard 2000; Ebert & Kleman 2004; Knudsen *et al.* 2006; Evans 2009; Hibbard *et al.* 2021). In the Teriberka IMZ, several sedimentary studies of the ring and ridge hummocky moraines identify conformable draped layers of fluviably redistributed sands, pebbles, and diamicton with occasional rounded cobbles and boulders (Yevzerov 2015; Vashkov & Nosova 2019; Vashkov 2020). Such deposits are interpreted as glacially transported sediments that have been subsequently redistributed into the ring and ridge morphology in a zone of melting dead ice (Yevzerov 2015; Vashkov &

Table 2. Relative age sequence of IMZ formation in NW Russia. Principles of morphostratigraphy, including instances of obliterative overlap, are used to place the reconstructed IMZs in a relative age sequence. In this relative chronology, horizontal lines separate IMZs that are known to be older or younger than each other; broken lines indicate an insecure relative chronology. Vertical lines separate IMZs that could be contemporaneous. Individual IMZs are not in a fixed position and can 'slide' up and down relative to laterally adjacent IMZs. Additionally, IMZs are not fixed to any defined time-span, with the length of different IMZ formation events probably fluctuating throughout a glacial cycle.

Older ↓ Younger	Salpausselkä I	Belomorsk					
	Rugozero						
	Salpausselkä II		Tuloma	Khibiny	Teriberka	Kola	Umba
	Kalevala		Kolvitsky		Monchetundra		
	Pyaozero		Karelide				

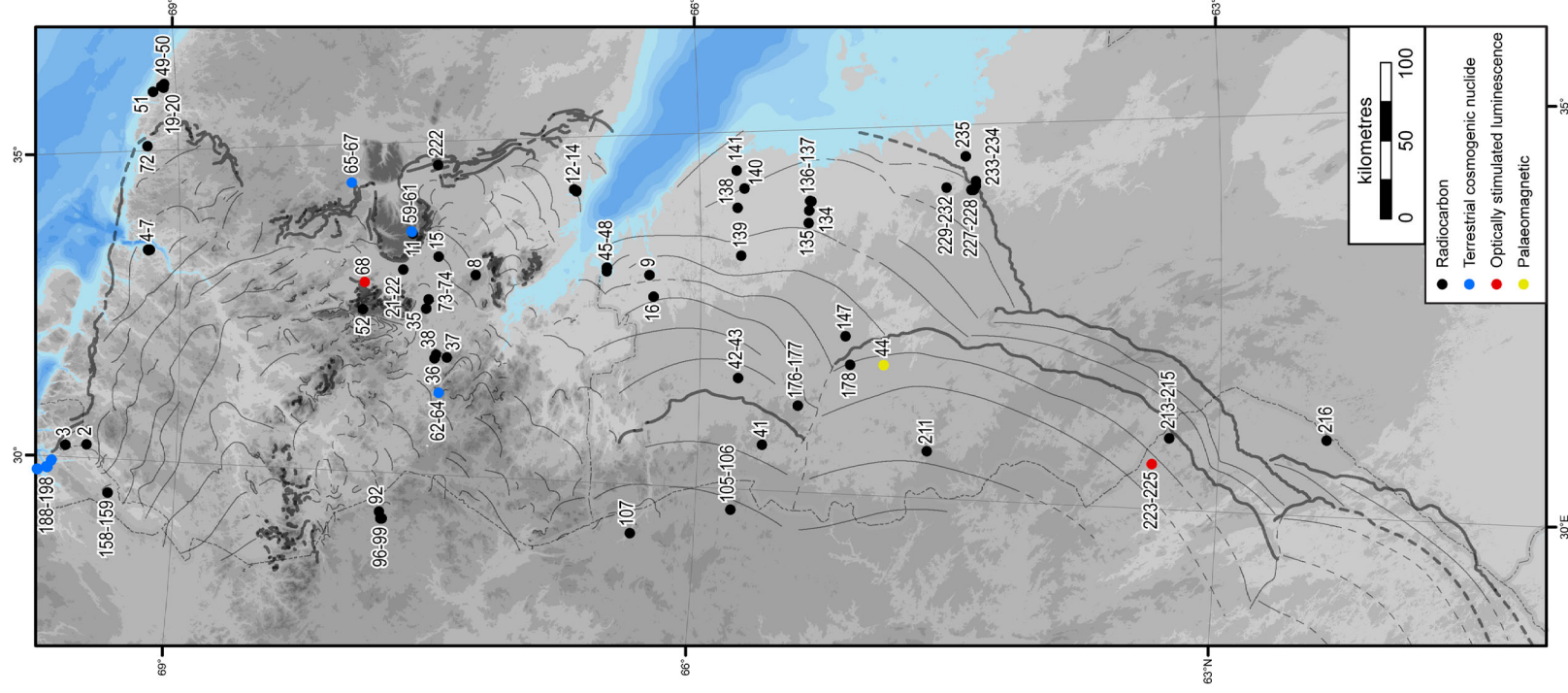


Fig. 5. Locations of numerical ages within the study area that are included in the numerical age database. Numerical ages outside of, and beyond, the study area are not shown for clarity, but the locations of all numerical ages can be viewed in the Supporting Information as Data S1 and S2.

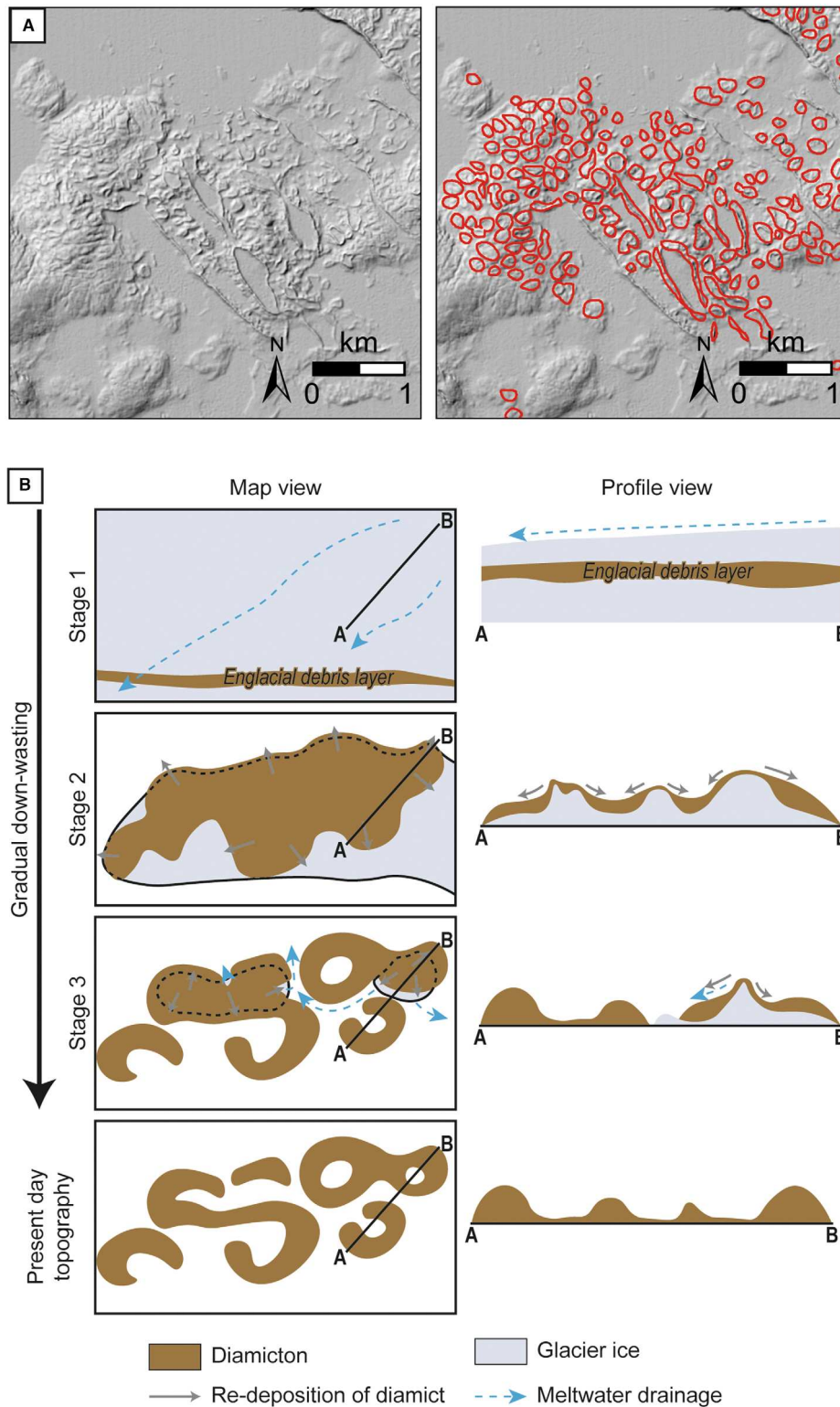


Fig. 6. Formational model for ring and ridge (Type 2a; Boyes *et al.* 2021b) hummocky moraines. A. An example of ring and ridge hummocky moraines from the Teriberka IMZ in the ArcticDEM (Porter *et al.* 2018; Boyes *et al.* 2021b). B. Englacial debris (Stage 1) is outcropped as the ice surface thins. Over time stagnated glacial ice under a layer of now supraglacial diamict will down-waste and separate into individual ice blocks (Stage 2–3). This now supraglacial debris is transferred away from topographic highs and deposited in topographic lows via mass movement and meltwater action. Unequal melt rates displace debris around extant dead-ice blocks. As a result, once all the ice has ablated, the present-day topography leaves a series of rings, ridges, and troughs (modified from Ebert & Kleman 2004 and Knudsen *et al.* 2006).

Nosova 2019; Vashkov 2020). With the supporting sedimentary evidence from the study area, the latter formational model is preferred here. On the Kola Peninsula, ring and ridge hummocky moraines are not always associated with subglacial bedforms and eskers (the latter of which are indicative of warm-based thermal regime flow events). Therefore, these moraines may be associated with a cold-based thermal regime ice margin, which is typical in subpolar glacial landsystems such as the Kola Peninsula (Sollid & Sørbel 1988). However, on the southern Kola Peninsula, chaotic hummocky moraine complexes surrounding end moraines of the Umba IMZ – which is located at the lateral margins of the Kanozero Ice Stream (Fig. 3; Boyes *et al.* 2023b) – may suggest downwasting ice margins following the collapse of the ice stream. Alternatively, the position of the Umba IMZ alongside the Kanozero Ice Stream may be coincidental, and instead, the Umba IMZ may also represent a cold-based ice-margin readvance like those observed on the northern Kola Peninsula.

The distinction between subpolar and temperate Younger Dryas stadial glacial landsystems across the study area is stark. However, this is consistent with the pre-Younger Dryas stadial glacial history of NW Russia. Hättstrand and Clark (2006b) and Boyes *et al.* (2023b) find that the FIS was predominantly cold-based on the Kola Peninsula throughout the last glaciation, which is consistent with the subpolar glacial landsystem. In contrast, Larsen *et al.* (2014) suggest that pre-Younger Dryas FIS glaciation below the Arctic Circle in NW Russia was driven, to a large extent, by pressurized subglacial meltwater; this is typical of temperate glacial landsystems. Such consistency of evidence for distinct glacial landsystems north and south of the Arctic Circle in NW Russia suggests that glaciation styles in NW Russia during the Younger Dryas stadial, and probably throughout the last glaciation, are inherently linked with climate and the geographic location of this region across the Arctic Circle divide.

Ice-sheet thickness and the topography of Murmansk Oblast also probably had a significant influence on the morphology of the Younger Dryas stadial FIS. The crenulated Teriberka IMZ that reflects contours in the landscape indicates that this cold-based ice-margin readvance occupied topographic lows. This in turn suggests that the ice sheet was characterized by low surface gradients and thus controlled by topographic thresholds (Larsen *et al.* 2014). This is especially apparent at the Khibiny IMZ, which indicates that ice lobes flowed around the Khibiny Mountains and a relatively thin ice sheet that was unable to flow into the massif. The low surface gradient of the FIS on the Kola Peninsula may have been influenced, in part, by the position of mountainous basal topography upstream. Based on the surface profiles of contemporary ice sheets, Boyes *et al.* (2023b) suggest that the summits of the Monchetundra and Chunutundra massifs were exposed as

nunataks during the Younger Dryas stadial. However, their reconstruction does not consider the influence that nunataks can exert on upstream and downstream ice-sheet thickness. For example, numerical modelling work by Mas e Braga *et al.* (2021) finds that a single nunatak can influence ice thickness >20 km away from its summit, with the most prominent effect being a local increase – on the order of hundreds of metres of ice surface elevation change – upstream of the obstacle. Conversely, Mas e Braga *et al.* (2021) observe an ice surface elevation decrease of similar magnitude downstream of an obstacle. The Monchetundra and Chunutundra mountains are dominant topographic features of the landscape, with an elevation prominence up to 800 m along a >50 km north–south aligned massif that was probably perpendicular to ice flow (Boyes *et al.* 2023a). Thus, it is conceivable that there was a lower ice surface elevation on the eastern (downstream) flanks of the Monchetundra and Chunutundra mountains and, accordingly, that the Monchetundra IMZ was formed contemporaneously with the Khibiny IMZ. However, such palaeo-inferences cannot be deduced from the geomorphological record; instead, numerical dating of the IMZs and on the massifs would be needed to verify this.

Although robust chronologies are lacking, it is likely that ice-margin retreat was rapid in NW Russia during the Early Holocene. Rapid ice-sheet retreat is a possible consequence of extensive but thin ice margins in NW Russia. Larsen *et al.* (2014), Stroeven *et al.* (2016) and Boyes *et al.* (2023b) suggest the FIS margin in Russia was characterized by low-gradient ice lobes that were situated in a precipitation shadow and sustained by steeper-gradient ice upstream. Moreover, these authors suggest that even minor fluctuations in ice-sheet mass balance could have significant consequences for ice-sheet dynamics in NW Russia. The overall negative mass balance of the FIS that is often associated with the Early Holocene glaciation (Stroeven *et al.* 2016; Patton *et al.* 2017) could have contributed to the rapid retreat of the ice margin in NW Russia by reducing the essential upstream ice mass inputs. However, rapid climatic warming, such as that experienced during the Younger Dryas–Early Holocene transition *c.* 11.7 ka, also probably induced melting of the FIS in NW Russia. In turn, the supply of meltwater to the subglacial environment – indicated by the extensive esker and subglacial meltwater channel networks across the study area – can accelerate the flow speed of an ice sheet and contribute to its retreat through increased ice mass outputs (Zwally *et al.* 2002; Stroeven *et al.* 2016; Patton *et al.* 2017; Shackleton *et al.* 2018).

The melting, subglacial meltwater drainage and associated retreat of palaeo-ice sheets produce several characteristic landform assemblages in the geomorphological record of the study area. First, a diverse meltwater landform assemblage – including abundant eskers,

subglacial meltwater channels and Type 3 hummocky moraine corridors – reveals channelized subglacial drainage networks (Greenwood *et al.* 2007; Storrar *et al.* 2014a; Lewington *et al.* 2020). Moreover, Lewington *et al.* (2020) suggest that Type 3 hummocky moraine corridors are indicative of fluctuations in hydraulic pressure in response to melt seasons, precipitation or supra/subglacial lake drainages. Second, the subglacial meltwater drainage networks are arranged in tracts hundreds of kilometres long. Such continuity suggests that meltwater drainage routes were time-transgressive features formed during stable and gradual retreat throughout deglaciation (Storrar *et al.* 2014b). Finally, abundant esker enlargements – braided complexes of esker ridges and glaciofluvial sediments (Dewald *et al.* 2021) – are identified on the proximal side of the Younger Dryas IMZs in the study area (Fig. 3B). Dewald *et al.* (2021), who mapped esker enlargements across the Nordic countries, suggest that esker enlargements are indicative of subglacial conduit collapse along high-discharge meltwater drainage routes in response to increased ablation under warmer climatic conditions. These authors propose that subglacial conduits collapse when the roof of a conduit becomes sufficiently thin, in response to (i) conduit growth, (ii) ice surface lowering, or (iii) a combination of both. The entire meltwater landform assemblage in the study area, especially in southern Karelia, is therefore indicative of (i) high volumes of subglacial meltwater discharge, which may have fluctuated in response to internal and external forces and (ii) considerable ice-sheet thinning, probably in response to climatic warming.

Speculative ice dynamics in NW Russia

In the previous section, we discussed the ice-sheet dynamics that are interpreted from the landform record of NW Russia. However, where the landform record is lacking, or processes of landform genesis are ambiguous, we speculate some additional ice-sheet dynamics that may have occurred in NW Russia. These speculations serve as hypotheses that should be tested in future research.

Reconstructions of IMZs and retreat patterns and interpretations of ice dynamics in the White Sea are currently prohibited by a lack of available data. For example, reconstruction of the Belomorsk IMZ is restricted to the contemporary terrestrial landscape, and the geomorphology is not as well preserved north of the Belomorsk IMZ. In addition, the offshore geomorphological evidence necessary for reconstructing the northward extension of this ice margin is lacking. Thus, the dynamics of the Kuusamo ice lobe (Fig. 3A) (which was probably operating as an ice stream; Boyes *et al.* 2023a) and its Younger Dryas IMZ are open to debate.

It is likely that the Kuusamo ice lobe terminated in an aquatic environment during the Younger Dryas. However, it is uncertain (i) whether this ice margin terminated in an ice-dammed lake (e.g. Pasanen *et al.* 2010; Lunkka

et al. 2012) or in a marine environment (e.g. Kolka *et al.* 2013a; Boyes 2022; Boyes *et al.* 2023b), or (ii) if the ice margin readvanced or retreated. Proglacial lakes can influence the subglacial hydrology of a glacier by interrupting subglacial meltwater drainage, thus elevating basal water pressures and encouraging glacier surging, especially where the glacier is topographically confined (Clayton *et al.* 1985; Lovell *et al.* 2012; Carrivick & Tweed 2013; Larsen *et al.* 2014). Very large proglacial lakes, such as that proposed for the White Sea basin (Pasanen *et al.* 2010; Lunkka *et al.* 2012), can also moderate local summer air temperatures and relatively retard summer ice ablation (Carrivick & Tweed 2013), potentially exacerbating climatic cooling associated with the Younger Dryas. As such, a combination of climate-driven ice expansion and secondary internal and external feedbacks may have induced a Kuusamo ice lobe readvance. Alternatively, marine transgression into the White Sea basin prior to the Younger Dryas stadial (Boyes 2022; Boyes *et al.* 2023b) may have facilitated warm ocean water incursion. When coupled with a decrease in meltwater outputs and changing insolation throughout the Younger Dryas stadial (Rinterknecht *et al.* 2014; Oksman *et al.* 2017), the FIS margin may have terminated in a relatively warm marine environment. As such, it is possible that the Kuusamo ice lobe was retreating during the Younger Dryas under the influence of warmer sea waters. However, aquatic terminating glaciers are complex systems, hence detailed geomorphological mapping, numerical dating and palaeoenvironmental reconstructions of the White Sea basin are needed to verify these theories.

Above we proposed that rapid climatic warming and associated melting of the FIS, indicated by the extensive subglacial drainage systems and numerous esker enlargements, resulted in the rapid retreat of the ice margin during the Early Holocene. A further mechanism that can drive rapid ice-sheet melt is a low albedo ice surface. The internal rotational flow of ice sheets often results in the outcropping of internal ice layers (Bøggild *et al.* 2010; Wientjes & Oerlemans 2010). Where these internal layers are debris-rich the ice surface can be darkened, and thus the albedo lowered. As a response, the ice surface melt increases, which in turn lowers the ice surface albedo further (Bøggild *et al.* 2010; Wientjes & Oerlemans 2010; van As *et al.* 2013). This positive feedback can facilitate the retreat of an ice mass significantly and is observed increasingly at contemporary glaciers and ice sheets (Wientjes & Oerlemans 2010; Box *et al.* 2012; van As *et al.* 2013). Since ring and ridge hummocky moraines are considered to be derived from englacial debris (see above), it is likely that englacial debris-rich layers were exposed at the surface of the FIS in NW Russia and may have contributed to the demise of the ice sheet owing to a reduction in albedo as described above. Large spreads of ring and ridge hummocky moraines on the Kola Peninsula might suggest that a

lower albedo ice surface was present on the peninsula during the Younger Dryas–Early Holocene. However, quantitatively evaluating the extent of possible dark surfaces of palaeo-ice sheets is impractical as outcropping of dark ice layers may not have been spatially restricted to locations where ring and ridge hummocky moraines are mapped.

Conclusions

In this paper, we present the first consistent large-scale reconstruction of FIS dynamics in NW Russia during the Younger Dryas stadial and Early Holocene and provide an independent evidence-based assessment of IMZs and ice-sheet retreat patterns. Conclusions that can be drawn from the reconstruction include:

- Ice-marginal landform assemblages reveal 14 IMZs in the study area. Rather than indicating continuous FIS margin positions in NW Russia, the morphostratigraphic relationships between the IMZs suggest multiple stages of ice-margin standstills and/or readvances throughout the Younger Dryas and Early Holocene.
- Distinct landform assemblages across the study area suggest two glacial landsystems during the Younger Dryas. A subpolar glacial landsystem characterized by cold-based thermal regimes dominated the FIS north of the Arctic Circle. In contrast, a temperate glacial landsystem comprising readvancing ice lobes characterized the landscape south of the Arctic Circle.
- Abundant subglacial meltwater channels and eskers across the study area suggest FIS melting during retreat, and that the meltwater was routed to the subglacial environment. This melting was probably a response to climatic warming during the Early Holocene.

However, there are key outstanding uncertainties in the reconstruction that remain unresolved:

- The absolute ages of IMZ formation in NW Russia is poorly constrained. This is because the majority of the ages in the numerical age database are not targeted at the IMZs or glacial events (Fig. 5). We therefore recommend that future dating studies not only target the IMZs reconstructed in this study, but also collect samples from across the breadth of discrete IMZs so as to fully capture the absolute ages of IMZ formation.
- Owing to the lack of high-resolution bathymetry data, reconstructions of the White Sea basin are currently impossible. As a result, past researchers, including ourselves, have speculated on possible retreat patterns but have been unable to verify ice dynamics in this location. We therefore recommend that future studies focus on this basin to test existing theories of ice-sheet advance and retreat in the White Sea.

The palaeoglacial reconstruction presented here adds considerable detail to previous investigations. Importantly, the reconstruction shows that IMZ formation in NW Russia was not synchronous, supporting the previous interpretations by Putkinen (2011). Thus, it is inappropriate to describe the Younger Dryas extent of the FIS in NW Russia as a continuous IMZ. We therefore recommend that future studies of FIS dynamics consider that other sectors of the Younger Dryas IMZ may also have formed asynchronously.

The palaeoglacial reconstruction presented here also shows the complexity in the geomorphological record that is missed when using small-scale geomorphological data. For example, the reconstruction indicates that at landform scales the ice margin was crenulated across NW Russia, even where arcuate landform assemblages suggest that the ice sheet had a disregard for regional topography. The IMZ and ice-margin retreat pattern reconstruction presented here summarizes the wealth of geomorphological data in NW Russia at a scale suited to numerical ice-sheet simulations. Moreover, our reconstruction provides a framework for palaeoglaciological field investigations to target research at understudied locations by identifying key areas where future research should focus to constrain the timing of ice-sheet retreat.

Acknowledgements. – The Universities of Brighton and Sheffield are gratefully acknowledged for granting BMB Visiting Researcher status to undertake and complete this work. Niko Putkinen is thanked for sharing his insight into this study area. Anna Hughes and three anonymous reviewers are thanked for their comments that improved this manuscript.

Author contributions. – BMB conceived the original study, carried out the glacial inversion process, compiled the numerical age database, and led the overall manuscript development. All authors contributed to the preparation of the final manuscript.

Data availability statement. – The numerical age database and associated shapefiles are provided as supplementary data. Other data are available by request.

References

- Aartolahti, T. 1974: Ring ridge hummocky moraines in northern Finland. *Fennia* 134, 22 pp.
- Andersen, B. G. 1979: The deglaciation of Norway 15,000–10,000 BP. *Boreas* 8, 79–87.
- Andersen, B. G., Lundqvist, J. & Saarnisto, M. 1995a: The Younger Dryas margin of the Scandinavian Ice Sheet – an introduction. *Quaternary International* 28, 145–146.
- Andersen, B. G., Mangerud, J., Sørensen, R., Reite, A., Sveian, H., Thoresen, M. & Bergström, B. 1995b: Younger Dryas ice-marginal deposits in Norway. *Quaternary International* 28, 147–169.
- van As, D., Fausto, R. S., Colgan, W. T., Box, J. E. & Promice project team 2013: Darkening of the Greenland ice sheet due to the melt albedo feedback observed at PROMICE weather stations. *GEUS Bulletin* 28, 69–72.
- Astakhov, V. I., Shkatova, V. K., Zastozhnov, A. S. & Chuyko, M. 2016: Glaciomorphological map of The Russian Federation. *Quaternary International* 420, 4–14.

- Bakke, J., Dahl, S. O., Paasche, Ø., Løvlie, R. & Nesje, A. 2005: Glacial fluctuations, equilibrium-line altitudes and palaeoclimate in Lyngen, northern Norway, during the Lateglacial and Holocene. *The Holocene* 15, 518–540.
- Barr, I. D. & Lovell, H. 2014: A review of topographic controls on moraine distribution. *Geomorphology* 226, 44–64.
- Bitinas, A. 2012: New insights into the last deglaciation of the south-eastern flank of the Scandinavian Ice Sheet. *Quaternary Science Reviews* 44, 69–80.
- Bøggild, C. E., Brandt, R. E., Brown, K. J. & Warren, S. G. 2010: The ablation zone in northeast Greenland: ice types, albedos and impurities. *Journal of Glaciology* 56, 101–113.
- Boone, S. J. & Eyles, N. 2001: Geotechnical model for great plains hummocky moraine formed by till deformation below stagnant ice. *Geomorphology* 38, 109–124.
- Boulton, G. S., Dongelmans, P., Punkari, M. & Broadgate, M. 2001: Palaeoglaciation of an ice sheet through a glacial cycle: the European ice sheet through the Weichselian. *Quaternary Science Reviews* 20, 591–625.
- Box, J. E., Fettweis, X., Stroeve, J. C., Tedesco, M., Hall, D. K. & Steffen, K. 2012: Greenland ice sheet albedo feedback: thermodynamics and atmospheric drivers. *The Cryosphere* 6, 821–839.
- Boyes, B. M. 2022: *The Last Fennoscandian Ice Sheet: A Palaeo-Glaciological Reconstruction on the Kola Peninsula and Russian Lapland*. 362 pp. School of Applied Sciences, University of Brighton, Brighton and Hove.
- Boyes, B. M. & Pearce, D. M. 2023: Glacial geomorphology of the Republic of Karelia, northwest Russia: the Younger Dryas-early Holocene ice marginal zone. *Journal of Maps* 19, 2230999, <https://doi.org/10.1080/17445647.2023.2230999>.
- Boyes, B. M., Linch, L. D., Pearce, D. M., Kolka, V. V. & Nash, D. J. 2021a: The Kola Peninsula and Russian Lapland: a review of Late Weichselian glaciation. *Quaternary Science Reviews* 267, 107087, <https://doi.org/10.1016/j.quascirev.2021.107087>.
- Boyes, B. M., Linch, L. D., Pearce, D. M. & Nash, D. J. 2023a: The last Fennoscandian Ice Sheet glaciation on the Kola Peninsula and Russian Lapland (Part 1): ice flow configuration. *Quaternary Science Reviews* 300, 107871, <https://doi.org/10.1016/j.quascirev.2022.107871>.
- Boyes, B. M., Linch, L. D., Pearce, D. M. & Nash, D. J. 2023b: The last Fennoscandian Ice Sheet glaciation on the Kola Peninsula and Russian Lapland (Part 2): ice sheet margin positions, evolution, and dynamics. *Quaternary Science Reviews* 300, 107872, <https://doi.org/10.1016/j.quascirev.2022.107872>.
- Boyes, B. M., Pearce, D. M. & Linch, L. D. 2021b: Glacial geomorphology of the Kola Peninsula and Russian Lapland. *Journal of Maps* 17, 497–515.
- Bryson, R. A., Wendland, W. M., Ives, J. D. & Andrews, J. T. 1969: Radiocarbon isochrones on the disintegration of the Laurentide Ice Sheet. *Arctic and Alpine Research* 1, 1–13.
- Carrivick, J. L. & Tweed, F. S. 2013: Proglacial lakes: character, behaviour and geological importance. *Quaternary Science Reviews* 78, 34–52.
- Clark, C. D., Hughes, A. L. C., Greenwood, S. L., Jordan, C. J. & Sejrup, H. P. 2012: Pattern and timing of retreat of the last British-Irish Ice Sheet. *Quaternary Science Reviews* 44, 112–146.
- Clayton, L. E. E., Teller, J. T. & Attig, J. W. 1985: Surging of the southwestern part of the Laurentide Ice Sheet. *Boreas* 14, 235–241.
- Darvill, C. M., Stokes, C. R., Bentley, M. J., Evans, D. J. A. & Lovell, H. 2017: Dynamics of former ice lobes of the southernmost Patagonian Ice Sheet based on a glacial landystems approach. *Journal of Quaternary Science* 32, 857–876.
- Dewald, N., Lewington, E. L. M., Livingstone, S. J., Clark, C. D. & Storrar, R. D. 2021: Distribution, characteristics and formation of esker enlargements. *Geomorphology* 392, 107919, <https://doi.org/10.1016/j.geomorph.2021.107919>.
- Dulfer, H. E., Margold, M., Darvill, C. M. & Stroeven, A. P. 2022: Reconstructing the advance and retreat dynamics of the central sector of the last Cordilleran Ice Sheet. *Quaternary Science Reviews* 284, 107465, <https://doi.org/10.1016/j.quascirev.2022.107465>.
- Ebert, K. & Kleman, J. 2004: Circular moraine features on the Varanger Peninsula, northern Norway, and their possible relation to polythermal ice sheet coverage. *Geomorphology* 62, 159–168.
- Ekman, I. & Iljin, V. 1991: Deglaciation, the Younger Dryas end moraines and their correlation in the Karelian A.S.S.R and adjacent areas. In Rainio, H. & Saarnisto, M. (eds.): *IGCP Project 253, Termination of the Pleistocene. Eastern Fennoscandian Younger Dryas End Moraines. Field Conference North Karelia, Geological Survey of Finland, Guide, 32, Finland and Karelian ASSR*, 73–99. Geological Survey of Finland, Espo.
- European Space Agency 2021: *Copernicus Global Digital Elevation Model. OpenTopography*.
- Evans, D. J. A. 2009: Controlled moraines: origins, characteristics and palaeoglaciological implications. *Quaternary Science Reviews* 28, 183–208.
- Evans, D. J. A. & Orton, C. 2015: Heinabergsjökull and Skalfellsjökull, Iceland: active temperate piedmont lobe and outwash head glacial landsystem. *Journal of Maps* 11, 415–431.
- Evans, D. J. A. & Twigg, D. R. 2002: The active temperate glacial landsystem: a model based on Breiðamerkurjökull and Fjallsjökull, Iceland. *Quaternary Science Reviews* 21, 2143–2177.
- Evans, D. J. A., Twigg, D. R., Rea, B. R. & Orton, C. 2009: Surging glacier landsystem of Tungnaárjökull, Iceland. *Journal of Maps* 5, 134–151.
- Evans, D. J. A., Twigg, D. R., Rea, B. R. & Shand, M. 2007: Surficial geology and geomorphology of the Brúarjökull surging glacier landsystem. *Journal of Maps* 3, 349–367.
- GEBCO Compilation Group 2023: GEBCO 2023 Grid. Available at <https://doi.org/10.5285/f98b053b-0c9c-6c23-e053-6c86abc0af7b> (accessed 01.06.2023).
- Gibbons, A. B., Megeath, J. D. & Pierce, K. L. 1984: Probability of moraine survival in a succession of glacial advances. *Geology* 12, 327–330.
- Gravenor, C. P. & Kupsch, W. O. 1959: Ice-disintegration features in Western Canada. *The Journal of Geology* 67, 48–64.
- Greenwood, S. L., Clark, C. D. & Hughes, A. L. C. 2007: Formalising an inversion methodology for reconstructing ice-sheet retreat patterns from meltwater channels: application to the British Ice Sheet. *Journal of Quaternary Science* 22, 637–645.
- Grosswald, M. G. 1980: Late Weichselian ice-sheet of northern Eurasia. *Quaternary Research* 13, 1–32.
- Grosswald, M. G. 2001: The Late Weichselian Barents-Kara Ice Sheet: in defense of a maximum reconstruction. *Russian Journal of Earth Sciences* 3, 427–452.
- Grosswald, M. G. & Hughes, T. J. 2002: The Russian component of an Arctic Ice Sheet during the Last Glacial Maximum. *Quaternary Science Reviews* 21, 121–146.
- Hättestrand, C. & Clark, C. D. 2006a: The glacial geomorphology of Kola Peninsula and adjacent areas in Murmansk Region, Russia. *Journal of Maps* 2, 30–42.
- Hättestrand, C. & Clark, C. D. 2006b: Reconstructing the pattern and style of deglaciation of Kola Peninsula, northeastern Fennoscandian Ice Sheet. In Knight, P. G. (ed.): *Glacier Science and Environmental Change*, 199–201. Blackwell Publishing, Oxford.
- Hättestrand, C., Kolka, V. V. & Johansen, N. 2008: Cirque infills in the Khibiny Mountains, Kola Peninsula, Russia – palaeoglaciological interpretations and modern analogues in East Antarctica. *Journal of Quaternary Science* 23, 165–174.
- Heaton, T. J., Köhler, P., Butzin, M., Bard, E., Reimer, R. W., Austin, W. E. N., Bronk Ramsey, C., Grootes, P. M., Hughen, K. A., Kromer, B., Reimer, P. J., Adkins, J., Burke, A., Cook, M. S., Olsen, J. & Skinner, L. C. 2020: Marine20 – the marine radiocarbon age calibration curve (0–55,000 cal BP). *Radiocarbon* 62, 779–820.
- Heyman, J. & Hättestrand, C. 2006: Morphology, distribution and formation of relict marginal moraines in the Swedish mountains. *Geografiska Annaler. Series A, Physical Geography* 88, 253–265.
- Hibbard, S. M., Osinski, G. R. & Godin, E. 2021: Vermicular ridge features on Dundas Harbour, Devon Island, Nunavut. *Geomorphology* 395, 107947, <https://doi.org/10.1016/j.geomorph.2021.107947>.
- Hoppe, G. 1952: Hummocky moraine regions with special reference to the interior of Norrbotten. *Geografiska Annaler* 34, 1–72.
- Hughes, A. L. C., Gyllencreutz, R., Lohne, O. S., Mangerud, J. & Svendsen, J. I. 2016: The last Eurasian ice sheets – a chronological database and time-slice reconstruction, DATED-1. *Boreas* 45, 1–45.

- Johnson, M. D., Mickelson, D. M., Clayton, L. E. E. & Attig, J. W. 1995: Composition and genesis of glacial hummocks, western Wisconsin, USA. *Boreas* 24, 97–116.
- Johnson, M. D., Wedel, P. O., Benediktsson, Í. Ö. & Lenninger, A. 2019: Younger Dryas glaciomarine sedimentation, push-moraine formation and ice-margin behavior in the Middle Swedish end-moraine zone west of Billingen, central Sweden. *Quaternary Science Reviews* 224, 105913, <https://doi.org/10.1016/j.quascirev.2019.105913>.
- Kirkbride, M. P. & Winkler, S. 2012: Correlation of Late Quaternary moraines: impact of climate variability, glacier response, and chronological resolution. *Quaternary Science Reviews* 46, 1–29.
- Kleman, J. & Borgström, I. 1996: Reconstruction of palaeo-ice sheets: the use of geomorphological data. *Earth Surface Processes and Landforms* 21, 893–909.
- Kleman, J., Hättetrand, C., Borgström, I. & Stroeven, A. P. 1997: Fennoscandian palaeoglaciology reconstructed using a glacial geological inversion model. *Journal of Glaciology* 43, 283–299.
- Kleman, J., Hättetrand, C., Stroeven, A. P., Jansson, K. N., De Angelis, H. & Borgström, I. 2006: Reconstruction of palaeo-ice sheets – inversion of their glacial geomorphological record. In Knight, P. G. (ed.): *Glacier Science and Environmental Change*, 192–198. Blackwell Science Ltd., Oxford.
- Knudsen, C. G., Larsen, E., Sejrup, H. P. & Stalsberg, K. 2006: Hummocky moraine landscape on Jæren, SW Norway – implications for glacier dynamics during the last deglaciation. *Geomorphology* 77, 153–168.
- Kolka, V. V., Korsakova, O. P., Shelekhova, T. S. & Arslanov, K. A. 2013a: Reconstruction of the relative sea level of the White Sea during the Holocene on the Karelian Coast near Engozero Settlement, northern Karelia. *Doklady Earth Sciences* 449, 434–438.
- Kolka, V. V., Yevzerov, V. Y., Møller, J. J. & Corner, G. D. 2013b: The Late Weichselian and Holocene relative sea-level change and isolation basin stratigraphy at the Umba settlement, southern coast of Kola Peninsula. *News of the Russian Academy of Sciences. Geographical Series* 1, 73–88 (in Russian).
- Kurimo, H. 1982: Ice-lobe formation and function during the deglaciation in Finland and adjacent Soviet Karelia. *Boreas* 11, 59–77.
- Kurjański, B., Rea, B. R., Spagnolo, M., Cornwell, D. G., Howell, J., Comte, J.-C., González-Quirós, A., Palmu, J.-P., Oien, R. P. & Gibbard, P. L. 2021: Cool deltas: sedimentological, geomorphological and geophysical characterization of ice-contact deltas and implications for their reservoir properties (Salpausselkä, Finland). *Sedimentology* 68, 3057–3101.
- Lagerbäck, R. 1988: The Veiki moraines in northern Sweden – widespread evidence of an Early Weichselian deglaciation. *Boreas* 17, 469–486.
- Lamsters, K. & Zelčs, V. 2015: Subglacial bedforms of the Zemgale Ice Lobe, south-eastern Baltic. *Quaternary International* 386, 42–54.
- Larsen, E., Fredin, O., Jensen, M. A., Kuznetsov, D., Lyså, A. & Subetto, D. A. 2014: Subglacial sediment, proglacial lake-level and topographic controls on ice extent and lobe geometries during the Last Glacial Maximum in NW Russia. *Quaternary Science Reviews* 92, 369–387.
- Lavrova, M. A. 1960: *Quaternary Geology of the Kola Peninsula*. 220 pp. Academia Science Press, Moscow-Leningrad (in Russian).
- Lewington, E. L. M., Livingstone, S. J., Clark, C. D., Sole, A. J. & Storrar, R. D. 2020: A model for interaction between conduits and surrounding hydraulically connected distributed drainage based on geomorphological evidence from Keewatin, Canada. *The Cryosphere* 14, 2949–2976.
- Lovell, H., Stokes, C. R., Bentley, M. J. & Benn, D. I. 2012: Evidence for rapid ice flow and proglacial lake evolution around the central Strait of Magellan region, southernmost Patagonia. *Journal of Quaternary Science* 27, 625–638.
- Lundqvist, J. 1995: The Younger Dryas ice-marginal zone in Sweden. *Quaternary International* 28, 171–176.
- Lunkka, J. P., Kaparullina, E., Putkinen, N. & Saarnisto, M. 2018: Late Pleistocene palaeoenvironments and the last deglaciation on the Kola Peninsula, Russia. *Arktos* 4, 1–18.
- Lunkka, J. P., Palmu, J.-P. & Seppänen, A. 2021: Deglaciation dynamics of the Scandinavian Ice Sheet in the Salpausselkä zone, southern Finland. *Boreas* 50, 404–418.
- Lunkka, J. P., Putkinen, N. & Miettinen, A. 2012: Shoreline displacement in the Belomorsk area, NW Russia during the Younger Dryas Stadial. *Quaternary Science Reviews* 37, 26–37.
- Mangerud, J. 2021: The discovery of the Younger Dryas, and comments on the current meaning and usage of the term. *Boreas* 50, 1–5.
- Mangerud, J., Aarseth, I., Hughes, A. L. C., Lohne, Ø. S., Skår, K., Sønstegeard, E. & Svendsen, J. I. 2016: A major re-growth of the Scandinavian Ice Sheet in western Norway during Allerød-Younger Dryas. *Quaternary Science Reviews* 132, 175–205.
- Mangerud, J., Hughes, A. L. C., Sæle, T. H. & Svendsen, J. I. 2019: Ice-flow patterns and precise timing of ice sheet retreat across a dissected fjord landscape in western Norway. *Quaternary Science Reviews* 214, 139–163.
- Mas e Braga, M., Selwyn Jones, R., Newall, J. C. H., Rogozhina, I., Andersen, J. L., Lifton, N. A. & Stroeven, A. P. 2021: Nunataks as barriers to ice flow: implications for palaeo ice sheet reconstructions. *The Cryosphere* 15, 4929–4947.
- Mollard, J. D. 2000: Ice-shaped ring-forms in Western Canada: their airphoto expressions and manifold polygenetic origins. *Quaternary International* 68-71, 187–198.
- Niemelä, J., Ekman, I. & Lukashov, A. 1993: *Quaternary deposits of Finland and northwestern part of Russian Federation and their resources: Map at 1: 1,000,000*. Geological Survey of Finland and Institute of Geology, Karelian Science Centre of the Russian Academy of Sciences.
- Oksman, M., Weckström, K., Miettinen, A., Juggins, S., Divine, D. V., Jackson, R., Telford, R., Korsgaard, N. J. & Kucera, M. 2017: Younger Dryas ice margin retreat triggered by ocean surface warming in central-eastern Baffin Bay. *Nature Communications* 8, 1017, <https://doi.org/10.1038/s41467-017-01155-6>.
- Pasanen, A., Lunkka, J. P. & Putkinen, N. 2010: Reconstruction of the White Sea Basin during the late Younger Dryas. *Boreas* 39, 273–285.
- Patton, H., Hubbard, A. L., Andreassen, K., Auriac, A., Whitehouse, P. L., Stroeven, A. P., Shackleton, C., Winsborrow, M., Heyman, J. & Hall, A. M. 2017: Deglaciation of the Eurasian ice sheet complex. *Quaternary Science Reviews* 169, 148–172.
- Petrov, O. V., Morozov, A. F., Chepkasova, T. V., Kiselev, E. A., Zastrozhnov, A. S., Verbitsky, V. R., Strelnikov, S. I., Tarnograd, V. D., Shkatova, V. K., Krutkina, O. N., Minina, E. A., Astakhov, V. I., Borisov, B. A. & Gusev, E. A. 2014: *Map of Quaternary formations of the territory of The Russian Federation. Scale 1: 2 500 000*. Ministry of Natural Resources and Ecology of the Russian Federation (in Russian).
- Porter, C., Morin, P., Howat, I. M., Noh, M.-J., Bates, B., Peterman, K., Keesey, S., Schlenk, M., Gardiner, J., Tomko, K., Willis, M., Kelleher, C., Cloutier, M., Husby, E., Foga, S., Nakamura, H., Platson, M., Wethington, M., Williamson, C., Bauer, G., Enos, J., Arnold, G., Kramer, W., Becker, P., Doshi, A., D'Souza, C., Cummens, P., Laurier, F. & Bojesen, M. 2018: *ArcticDEM*. Available at: <https://doi.org/10.7910/DVN/OHHUKH>. Harvard Dataverse, V1 (accessed 01.11.2018).
- Punkari, M. 1980: The ice lobes of the Scandinavian ice sheet during the deglaciation in Finland. *Boreas* 9, 307–310.
- Punkari, M. 1982: Glacial geomorphology and dynamics in the eastern parts of the Baltic Shield interpreted using Landsat imagery. *Photogrammetric Journal of Finland* 9, 77–93.
- Punkari, M. 1985: Glacial geomorphology and dynamics in Soviet Karelia interpreted by means of satellite imagery. *Fennia* 163, 113–153.
- Punkari, M. 1993: Modelling of the dynamics of the Scandinavian ice sheet using remote sensing and GIS methods. In Aber, J. S. (ed.): *Glaciotectonics and Mapping Glacial Deposits: Proceedings of the INQUA Commission on Formation and Properties of Glacial Deposits*, 232–250. Canadian Plains Research Center, Regina.
- Punkari, M. 1995: Glacial flow systems in the zone of confluence between the Scandinavian and Novaya Zemlya ice sheets. *Quaternary Science Reviews* 14, 589–603.
- Punkari, M. 1997: Subglacial processes of the Scandinavian ice sheet in Fennoscandia inferred from flow-parallel features and lithostratigraphy. *Sedimentary Geology* 111, 263–283.
- Putkinen, N. 2011: *Late Weichselian Deglaciation Chronology and Palaeoenvironments in Northern Karelia, NW Russia*. 21 pp. Geological Survey of Finland, Espoo.

- Putkinen, N. & Lunkka, J. P. 2008: Ice stream behaviour and deglaciation of the Scandinavian Ice Sheet in the Kuititjärvi area, Russian Karelia. *Bulletin of the Geological Society of Finland* 80, 19–37.
- Putkinen, N., Lunkka, J. P., Ojala, A. E. K. & Kosonen, E. 2011: Deglaciation history and age estimate of the Younger Dryas end moraines in the Kalevala region, NW Russia. *Quaternary Science Reviews* 30, 3812–3822.
- Rainio, H. 1985: Pohjois-Karjalan Salpausselkien aikaiset reunamuodostumat tarvitsevat nimet. *Geologi* 37, 48–50.
- Rainio, H., Saarnisto, M. & Ekman, I. 1995: Younger Dryas end moraines in Finland and NW Russia. *Quaternary International* 28, 179–192.
- Rasmussen, S. O., Bigler, M., Blockley, S. P., Blunier, T., Buchardt, S. L., Clausen, H. B., Cvijanovic, I., Dahl-Jensen, D., Johnsen, S. J., Fischer, H., Gkinis, V., Guillevic, M., Hoek, W. Z., Lowe, J. J., Pedro, J. B., Popp, T., Seierstad, I. K., Steffensen, J. P., Svensson, A. M., Vallelonga, P., Vinther, B. M., Walker, M. J. C., Wheatley, J. J. & Winstrup, M. 2014: A stratigraphic framework for abrupt climatic changes during the Last Glacial period based on three synchronized Greenland ice-core records: refining and extending the INTIMATE event stratigraphy. *Quaternary Science Reviews* 106, 14–28.
- Regnéll, C., Briner, J. P., Hafliðason, H., Mangerud, J. & Svendsen, J. I. 2022: Deglaciation of the Scandinavian ice sheet and a Younger Dryas ice cap in the outer Hardangerfjorden area, southwestern Norway. *Boreas* 51, 255–273.
- Reimer, P. J. and 41 others 2020: The IntCal20 Northern Hemisphere radiocarbon age calibration curve (0–55 cal kBP). *Radiocarbon* 62, 1–33.
- Rinterknecht, V. R., Jomelli, V., Brunstein, D., Favier, V., Masson-Delmotte, V., Bourlès, D., Leanni, L. & Schläppy, R. 2014: Unstable ice stream in Greenland during the Younger Dryas cold event. *Geology* 42, 759–762.
- Salonen, V.-P. 1990: Salpausselkä III, Pertille. In Lundqvist, J. & Saarnisto, M. (eds.): *Termination of the Pleistocene*, 63–64. Geological Survey of Finland, Opas-Guide.
- Schomacker, A., Benediktsson, Í. Ó. & Ingólfsson, Ó. 2014: The Eyjabakkajökull glacial landsystem, Iceland: geomorphic impact of multiple surges. *Geomorphology* 218, 98–107.
- Shackleton, C., Patton, H., Hubbard, A. L., Winsborrow, M., Kingslake, J., Esteves, M., Andreassen, K. & Greenwood, S. L. 2018: Subglacial water storage and drainage beneath the Fennoscandian and Barents Sea ice sheets. *Quaternary Science Reviews* 201, 13–28.
- Sollid, J. L. & Sørbel, L. 1988: Influence of temperature conditions in formation of end moraines in Fennoscandia and Svalbard. *Boreas* 17, 553–558.
- Stokes, C. R., Tarasov, L., Blomdin, R., Cronin, T. M., Fisher, T. G., Gyllencreutz, R., Hättestrand, C., Heyman, J., Hindmarsh, R. C. A., Hughes, A. L. C., Jakobsson, M., Kirchner, N., Livingstone, S. J., Margold, M., Murton, J. B., Riko, N., Peltier, W. R., Petet, D. M., Piper, D. J. W., Preusser, F., Renssen, H., Roberts, D. H., Roche, D. M., Saint-Ange, F., Stroeven, A. P. & Teller, J. T. 2015: On the reconstruction of palaeo-ice sheets: recent advances and future challenges. *Quaternary Science Reviews* 125, 15–49.
- Storrar, R. D., Stokes, C. R. & Evans, D. J. A. 2014a: Increased channelization of subglacial drainage during deglaciation of the Laurentide ice sheet. *Geology* 42, 239–242.
- Storrar, R. D., Stokes, C. R. & Evans, D. J. A. 2014b: Morphometry and pattern of a large sample (>20,000) of Canadian eskers and implications for subglacial drainage beneath ice sheets. *Quaternary Science Reviews* 105, 1–25.
- Stroeven, A. P., Hättestrand, C., Kleman, J., Heyman, J., Fabel, D., Fredin, O., Goodfellow, B. W., Harbor, J. M., Jansen, J. D., Olsen, L., Caffee, M. W., Fink, D., Lundqvist, J., Rosqvist, G. C., Strömberg, B. & Jansson, K. N. 2016: Deglaciation of Fennoscandia. *Quaternary Science Reviews* 147, 91–121.
- Svendsen, J. I., Alexanderson, H., Astakhov, V. I., Demidov, I. N., Dowdeswell, J. A., Funder, S., Gataullin, V., Henriksen, M., Hjort, C., Houmark-Nielsen, M., Hubberten, H. W., Ingólfsson, Ó., Jakobsson, M., Kjær, K. H., Larsen, E., Lokrantz, H., Lunkka, J. P., Lyså, A., Mangerud, J., Matiouchkov, A., Murray, A., Möller, P., Niessen, F., Nikolskaya, O., Polyak, L., Saarnisto, M., Siegert, C., Siegert, M. J., Spielhagen, R. F. & Stein, R. 2004: Late quaternary ice sheet history of northern Eurasia. *Quaternary Science Reviews* 23, 1229–1271.
- Tolstobrova, A. N., Tolstobrov, D. S., Kolka, V. V. & Korsakova, O. P. 2016: Late glacial and postglacial history of Lake Osinovoye (Kola region) inferred from sedimentary diatom assemblages. *Proceedings of the Karelian Scientific Centre of the RAS* 5, 106–116 (in Russian).
- Vashkov, A. A. 2020: Structure of ice-marginal deposits of the last glaciation near Lake Perkhayvr (northern Kola Peninsula). *Proceedings of the Fersmanov Scientific Session of the State Institute of the KSC RAS* 17, 71–75 (in Russian).
- Vashkov, A. A. & Nosova, O. Y. 2019: The composition of ridge relief and deglaciation features in the area of Lake Martimyabr (Kola peninsula). *Vestnik VSU. Series: Geology* 2, 26–35 (in Russian).
- Wientjes, I. G. M. & Oerlemans, J. 2010: An explanation for the dark region in the western melt zone of the Greenland Ice Sheet. *The Cryosphere* 4, 261–268.
- Wittmeier, H. E., Schaefer, J. M., Bakke, J., Rupper, S., Paasche, Ø., Schwartz, R. & Finkel, R. C. 2020: Late Glacial mountain glacier culmination in Arctic Norway prior to the Younger Dryas. *Quaternary Science Reviews* 245, 106461, <https://doi.org/10.1016/j.quascirev.2020.106461>.
- Yevzerov, V. Y. 2001: Valdai (Weichselian) glaciation in the Kola Region. In Matishov, G. G., Denisov, V. V., Dzhenyuk, S. L. & Tarasov, G. A. (eds.): *Problems and Methods of Ecological Monitoring of the Seas and Coastal Zones of the Western Arctic Regions*, 20–33. Kola Science Centre, Apatity (in Russian).
- Yevzerov, V. Y. 2015: The structure and formation of the outer strip of one of the marginal belts of the Late Valdaian ice sheet in the Kola region. *Vestnik VSU. Series: Geology* 4, 5–12 (in Russian).
- Yevzerov, V. Y. 2018: On the influence of latitudinal climatic zonation on the degradation of the Late Valdai (Late Visla) glaciation with the example of marginal formations on the territories of Finland and Karelian-Kola region. *Reports of Geological Institute of KCS RAS* 21, 18–25 (in Russian).
- Yevzerov, V. Y. & Kolka, V. V. 1993: End moraines of Younger Dryas and deglaciation of northern and central Kola Peninsula. In Yevzerov, V. Y. (ed.): *Eastern Fennoscandian Younger Dryas End Moraines and Deglaciation. Excursion Guide*, 5–38. Kola Science Centre RAS, Apatity (in Russian).
- Yevzerov, V. Y. & Nikolaeva, S. B. 2000: Marginal belts of the Kola region. *Geomorphology (Moscow)* 1, 61–73 (in Russian).
- Zwally, H. J., Abdalati, W., Herring, T., Larson, K., Saba, J. & Steffen, K. 2002: Surface melt-induced acceleration of Greenland Ice-Sheet flow. *Science* 297, 218–222.

Supporting Information

Additional Supporting Information to this article is available at <http://www.boreas.dk>.

Data S1. Numerical age database. Radiocarbon, luminescence, terrestrial cosmogenic nuclide and palaeomagnetic age data used to constrain the Fennoscandian Ice Sheet glaciation chronology.

Data S2. Shapefiles and associated files for the numerical age database used to constrain the Fennoscandian Ice Sheet glaciation chronology.

Data S3. Numerical age database references.